minerals

MDPI

Article

Geochemistry, Mineralogy and Textural Properties of the Lower Globigerina Limestone Used in the Built Heritage

Lino Bianco [1,2]

[1] Faculty for the Built Environment, University of Malta, MSD 2080 Msida, Malta; lino.bianco@um.edu.mt
[2] Faculty of Architecture, University of Architecture, Civil Engineering and Geodesy, 1 Hristo Smirnenski Blvd., 1046 Sofia, Bulgaria

Abstract: The Lower Globigerina Limestone Member, the oldest member of the Globigerina Limestone Formation, outcrops over most of the Maltese archipelago, notably Malta. It has provided the islands' main building material since the Neolithic period. This paper makes available a corpus of findings relating to the geochemistry, mineralogy and textural properties of this limestone—mostly unpublished and undertaken nearly three decades ago—which provide a useful source to understand its behavior. Bulk chemistry and mineralogy showed that non-carbonate and clay content is higher in limestone of inferior quality. Textural analyses gave insight into the fabric of the matrix, including inter- and intra-particle porosity. These analyses were supplemented by an array of petrophysical tests, including color (a parameter which has a correlation with density and Fe_2O_3 content), ultrasonic pulse velocity and compressive strength. The findings not only give insight into the composition of the limestone, using insoluble residue content of $\geq$5% as the threshold of inferior quality lithotype, but provided an insight into the physico-mechanical bonding present, a characteristic which has a bearing on the deterioration of this limestone.

Keywords: lower globigerina limestone; franka; sol; soll; Malta; physico-mechanical properties; limestone weathering; limestone durability; bioturbation; insoluble residue

Citation: Bianco, L. Geochemistry, Mineralogy and Textural Properties of the Lower Globigerina Limestone Used in the Built Heritage. *Minerals* **2021**, *11*, 740. https://doi.org/10.3390/min11070740

Academic Editors: Carmela Vaccaro and Elena Marrocchino

Received: 17 May 2021
Accepted: 25 June 2021
Published: 7 July 2021

1. Introduction

What primarily impressed the English poet Samuel Taylor Coleridge (1772–1834), when he travelled to Malta in 1804 for a two-year posting as undersecretary (and later public secretary) to the Civil Commissioner of Malta, was the shining buildings erected in "sand-free stone" around the Grand Harbour of Malta [1]. As Blouet recounts, "As he starts to explore Valletta and the urban environment around the harbors, Coleridge is bewildered at the Maltese use of limestone for every kind of construction—house, street, and wall—a centuries-old tradition born from the lack of other natural resources on the island [2]" [3] (p. 6).

The sand-free stone which Coleridge makes reference to is the Lower Globigerina Limestone (LGL), the honey-colored stone in which the built legacy of the Maltese Archipelago is realized (Figure 1). A description of the islands penned by Johannes Quintinus D'Autun (1500–1561) and published in Lyon in 1536, noted that masons in Malta "make good use of the island's stone for building purposes The Maltese stone is . . . remarkable for its softness; it is worked easily, but it is not strong enough against moistures and the sea-breeze" [4] (pp. 37–39).

The LGL is one of the soft limestones outcropping in the Mediterranean Basin. Often referred to as "Malta stone", it is the main industrial mineral terrestrial resource of the Maltese Islands. It is easy to quarry—it is "soft, and easy to cut into any shape" [5] (p. 46), and outcrops over two thirds of mainland Malta [6], the main island of the Maltese Archipelago. With a superficial area of approximately 316 km^2, this archipelago is located circa 93 km south of Sicily and 288 km north of Libya, and comprises several islands, the inhabited ones being Malta, Gozo and Comino.

Figure 1. The Maltese Archipelago: (**a**) location with respect to the Mediterranean Basin; (**b**) the main habitable islands; the location of case-studies is also included (© Google Earth).

1.1. Utilization of Lower Globigerina Limestone in Buildings

LGL has been quarried since the Neolithic period (3600–2500 BC), and is still the principal source of limestone for buildings on the Maltese Islands—whether for the construction of contemporary architectural and infrastructural works or for the restoration of built heritage. It was utilized by builders flourishing during one of the oldest Neolithic civilizations of the Mediterranean Basin [7–11]. Archeological structures dating from this period illustrate that those who built them differentiated between the softer, less durable LGL and the harder, denser, stronger and more durable varieties of Coralline Limestone (CL) used for external walls, which were uncarved. In contemporary minerals planning practice in Malta, LGL and CL are referred to softstone and hardstone, respectively.

Malta's numerous free-standing megalithic structures dating from the Neolithic period, a number of which are listed as UNESCO World Heritage sites [12] (Figure 2a) are examples of anthropogenic geodiversity *par excellence* [13]. The softness of LGL implies that it is easily hewed; as a result, there are many hypogea and catacombs carved into outcrops throughout the islands, most notably the Ħal Saflieni Hypogeum (c. 2500 BC) [14] and St Paul's Catacombs (early centuries of Christianity and used until seventh or eighth century AD) [15].

LGL was used in Mdina, the old capital city which originally formed part of the ancient of city of Melite (Greek: Μελίτη; Maleth under the Phoenicians [16]), and in Valletta, the Late Renaissance capital, which was founded in 1566. Laid out as a Hippodamian grid on a peninsula between two natural harbors [17], Valletta boasts an ensemble of 320 monuments within a superficial area of 55 ha (0.56 km^2) (Figure 2b). This entire area is registered as a UNESCO World Heritage Site [18]. LGL was used in Malta not only in buildings and monuments (see, for example, [19,20]), but also in the erection of fortifications surrounding Mdina [21], Valletta [22,23] and Cottonera [23]. The Hospitaller Order of St John (1530–1798) made extensive use of Globigerina limestone from local quarries throughout the duration of their stay [24,25].

The structural engineering properties of LGL were tested to the limit with the erection of the Neoclassical Rotunda of Mosta, one of the largest unsupported masonry domes in the history of building construction [26,27]. During the early years of the Order's presence in Malta, CL was used in the production of small works such as mill stones, with one such quarry operating in Birgu [28]. By the late seventeenth century, it was used at sites exposed to sea-spray. For example, the exterior walls of the bastions facing Marsamxett

Harbor were erected in CL, as directed by the Flemish architect and military engineer Carlo Grunenburg [22]. The lower part was constructed in dimension stones from highly durable CL extracted from the San Leonardo's Beds [29]. Hardstone from these beds was used for the drums of the columns of the gateways to the Grandmaster's Palace (Figure 2b), which were added in the mid-eighteenth century [29].

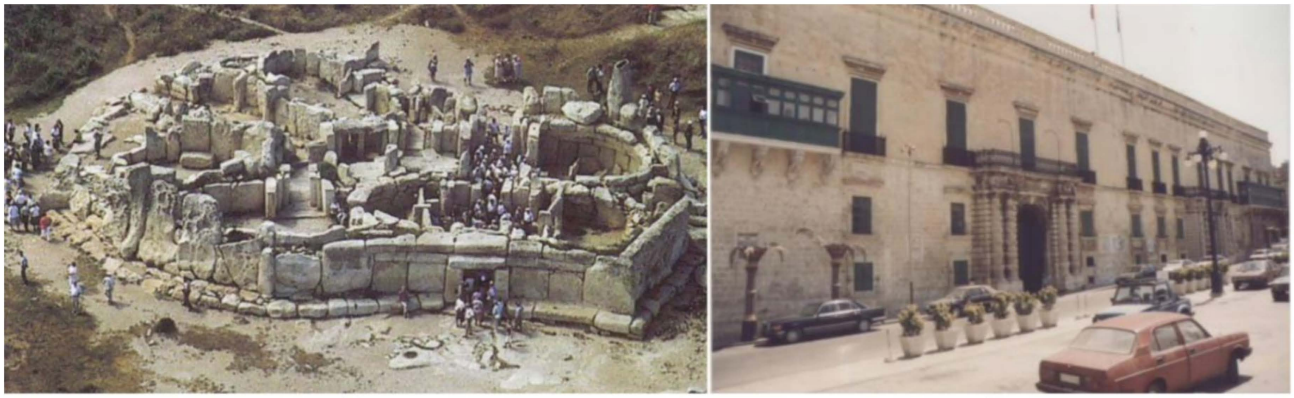

(a) (b)

Figure 2. Dated photo of: (**a**) Ħaġar Qim Neolithic Temples, Qrendi, one of the UNESCO World Heritage sites in Malta (Ħagar Qim by peuplier is licensed under CC BY 2.0) [30]; (**b**) the Grandmaster's Palace, Valletta.

During the British occupation of the islands (1800–1964), LGL was exported to other countries bordering the Mediterranean [31–33]. Noting the importance of this limestone for restoration and conservation of the cultural heritage of the islands, when applying for Malta's accession to the European Union, the Government of the Republic of Malta—which had prohibited the export of Maltese stone—put forward a case for the retention of the status quo in this regard [34]. An internal policy on the utilization of Malta stone was subsequently drafted—but never implemented—to conserve and regulate in situ mineral reserves of LGL suitable for the preservation of cultural patrimony [35]. Following a nomination by the University of Malta [36], LGL was designated as a Global Heritage Stone Resource in 2019, a designation supported by the International Union of Geological Sciences. Traditionally, the waste generated in quarrying and forming LGL dimension stones was negligible, as all was utilized as a product in the building industry: roughly cut stone as infill for walls, for levelling land and for sub-bases, whilst LGL powder was used in the production of mortar. LGL obtained from demolitions was often recycled for same uses. Today, it is utilized in polymer cement mortar [37,38] and reconstituted masonry products as an alternative to natural limestone and concrete blocks [39].

1.2. Aims of the Study

The author was the first who comprehensively studied Malta's LGL, as a topic for his Master's thesis in 1992–93 at the University of Leicester, UK, under the academic supervision of Dr Hugh Martyn Pedley [40]. The present article makes available the corpus data from this postgraduate research project, which has never been published in its entirety. It specifically addresses the geochemical, mineralogical, textural and physico-mechanical properties of LGL—all vital to understanding the behavior of this limestone. These properties are "useful for an integrated, holistic approach to natural limestone selection, a critical factor to identify sources either for stone replacement in . . . architecture or determine the preservation and/or conservation interventions required. They establish existing limestone resources compatible with the fabric used in a given monument" [41] (p. 9). They are of paramount importance in determining which limestone should be utilized in any conservation intervention on cultural heritage [42,43]. The aims of the study were to establish empirically whether (i) clay weakens the fabric and encourages weathering, (ii) bioturbation is a useful indicator to establish the quality of LGL, (iii) bioturbation introduces

weaknesses and unstable material into the fabric, and (iv) color and sound are indicators of quality of LGL. The study included discussions on natural weathering (subsequently published as [44]) and on the potential applications of limestone.

2. Geological Setting

2.1. General Lithostratigraphy

The earliest literature on the stratigraphy of the archipelago is from the nineteenth century [45–48]. This information was later restated in elementary geological texts [49–51]. Knowledge in this area was further refined in the second half of the twentieth century [52–55]. A new lithostratigraphical and palaeoenvironmental interpretation of the Coralline Limestone formations was published by Pedley [56].

The islands form part of the Pelagian Block, which extends from the Maltese Islands to eastern Tunisia and to the west of the Ionian Sea [57–59]. Situated on the eastern edge of the North African Pelagean Shelf, which is mainly calcareous and upper Triassic to late Tertiary in age, they lie on a submarine plateau that starts due south of the Ragusa Peninsula and extends to the coast of Libya and Tunisia. The depth of the shelf varies from around 90 m between Malta and Sicily, to over 1000 m before reaching the North Africa [55,60]. The shallower part of the shelf formed an epicontinental terrestrial link during the first epoch of the Quaternary, facilitating the migration of now extinct exotic fauna during the Pleistocene [61].

The stratigraphy of the islands is composed of five, mid-Tertiary, shallow marine carbonates, frequently fissured, Oligo-Miocene lithological formations, and facies capped with Quaternary deposits [6]. Ordered chronologically, starting from the earliest, the stratigraphy is composed of the following formations: Lower Coralline Limestone (LCL), Globigerina Limestone, Blue Clay, Greensand and the Upper Coralline Limestone. The stratigraphical sequence—which follows Rizzo [49] and Pedley [56]—and the corresponding thickness of the relative geological strata outcropping in Malta, is given in Table 1. The geological map of the Maltese Archipelago is reproduced in Figure 3. The LGL, the oldest member of the Globigerina Limestone Formation, is Aquitanian in age [53,62]. Isopachyte maps of the LGL are given in Pedley [63] and Pedley et al. [64]. A synthesis of the stratigraphic features of the archipelago is given in Baldassini and Di Stefano [65].

Table 1. The lithostratigraphy of the Maltese Archipelago [6].

Formation	Member	Age	Thickness (*t*) (m)	
			Malta	Gozo and Comino
Upper Coralline Limestone	Ġebel Imbark	Messinian	$04 \leq t \leq 25$	$04 \leq t \leq 20$
	Tal-Pitkal	Tortonian to Messinian	$30 \leq t \leq 50$	$01 \leq t \leq 30$
	Mtarfa	Tortonian	$12 \leq t \leq 16$	$02 \leq t \leq 16$
	Għajn Melel	Tortonian	$00 \leq t \leq 13$	$00 \leq t \leq 16$
Greensand		Tortonian		$00 \leq t \leq 11$
Blue Clay		Serravallian to Tortonian	$15 \leq t \leq 75$	$18 \leq t \leq 75$
Globigerina Limestone	Upper Globigerina Limestone	Langhian	$08 \leq t \leq 26$	$02 \leq t \leq 15$
	Middle Globigerina Limestone	Aquitanian to Burdigalian	$15 \leq t \leq 38$	$00 \leq t \leq 15$
	Lower Globigerina Limestone	Aquitanian	$00 \leq t \leq 80$	$05 \leq t \leq 40$
Lower Coralline Limestone	Il-Mara	Chattian	$00 \leq t \leq 20$	$00 \leq t \leq 06$
	Xlendi	Chattian	$00 \leq t \leq 22$	$00 \leq t \leq 22$
	Attard	Chattian	$10 \leq t \leq 15$	$10 \leq t \leq 15$
	Magħlaq	Chattian	$t > 38$	*t* unknown

2.2. Lithostratigraphic Outline of LGL

Lithological and paleontological features of LGL vary both laterally and vertically. A comprehensive and concise description of the lithostratigraphy is given in Baldassini et al. [66]. It is composed of massively bedded, pale yellow-brown biodetrital limestones (globigerinid biomicrosparites and biomicrites). Pale cream to yellow planktonic foraminiferal packstones quickly develop into wackestones above its base [6]. It consists mainly of globigerinid planktonic foraminifera. The color is less pale in the lower part of this member, which is coarser grained, yellow-brown and strongly bioturbated, in contrast with the upper part which is fine-grained, marly and light yellow. Macrofossils are abundant: bryozoans and the echinoid *Scutella* in the lower part, and pectinid bivalves (predominantly *Flabellipecten*) and echinoids (such as *Schizaster*) in the upper part [66,67]. *Scutella* biofacies (also referred to as "Scutella Bed" or "transitional Bed", consisting of a massive density of large flat echinoids, are present in the lowest part of the LGL member, with *Schizaster/Hemiaster* biofacies in the remaining part [68]. These biofacies mark the threshold between the LGL and the LCL formations, overlaying the latter. Recent research on the bio-chronostratigraphy of the LGL [66] follows the interpretation of a number of authors [53,69–71] who position this threshold on the upper surface of a ubiquitous hardground below the *Scutella* biofacies. A phosphatic bed—referred to as the "Basal Globigerina Limestone Phosphatic Bed" in Carbone et al. [70] and the "Terminal Lower Coralline Limestone Hardground" in Bennett [69,72]—covers this upper surface.

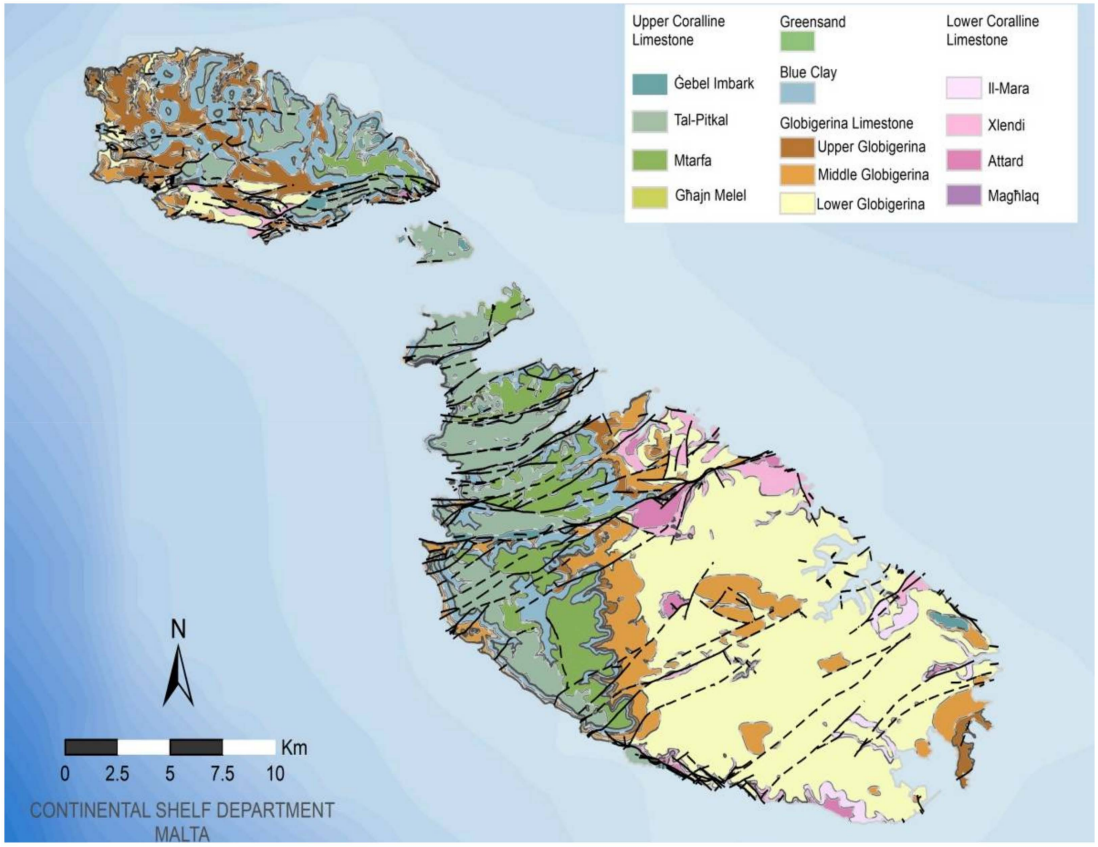

Figure 3. Geological map of the Maltese Islands [73].

The threshold between the LGL and the overlying Middle Globigerina Limestone Member (MGL) is marked by another ubiquitous hard bed, less than 1 m thick and rich in brown phosphatic nodules ("C1", or "Lower main conglomerate" in Pedley [54] and Pedley et al. [64]; "Qammieh bed" in Bennett [69]; "Lower Main Phosphorite Conglomerate Bed" in Pedley and Bennett [74]; "Qammieh Conglomerate Bed" in Rose et al. [71]). It marks an

interruption in sedimentation [74] and occurs at the top of the LGL and at the base of the MGL [74,75]. New preliminary data regarding the bio-chronostratigraphy of the LGL is based on calcareous plankton was published by Foresi et al. [67], placing the deposition of this member between 25.1 and 24.3 Ma [66].

2.3. Geochemistry, Mineralogy and Texture of LGL

A main scientific publication addressing this theme was penned by the eminent British oceanographer, Sir John Murray (1841–1914) [48]. His analysis and interpretation of the geology of the Malta Islands was the main source in all publications appearing until the late 1960s (e.g., [19,50]. In his work, Murray relied heavily on information furnished to him by Civil Engineer Charles Henry Colson (1864–1939) who, at the time, was engaged in the construction of a new dock in Malta, which became the theme of a paper—co-authored with his father Charles Colson—presented at the 1893–1894 session of the Institution of Civil Engineers [76]. Based on the communication with Colson, classifications of the numerous beds of Lower Coralline Limestone, Globigerina Limestone, Greensand and Upper Coralline Limestone were drawn up and cited as Murray [48] by Rizzo [49] when the latter tabulated the varying terminology coined for the stratigraphic beds by different authors [46,77], including his own, which was a refined version of Murray's. Based on this information from Colson, a classification of the strata occurring within the Globigerina Formation—inclusive of their diagnostic properties and respective uses in the building industry—was drawn up by Hughes [19]. The same information was used to tabulate, for all formations, a classification of all beds present, and their distinguishable characteristics and uses in Bianco [40] and published as Bianco [78].

The samples analyzed by Murray [48] from the Globigerina Formation had a $CaCO_3$ content between 63.20% and 94.73%; the upper beds had 30% to 40%. In most beds, $MgCO_3$ was present. All contained traces of $Ca_3(PO_4)_2$; it was 3% to 4% in some samples. The insoluble residue consisted of clayey matter and iron oxides, glauconite, and small mineral grains—namely, quartz splinters, feldspars, augite, zircon, tourmaline, rutile and hornblende—with sizes rarely >0.1 mm in diameter. These minerals are present in insignificant quantities in the Upper Globigerina Limestone Member [54]. No feldspar, augite and hornblende were identified in the LGL.

2.4. Terminology Associated with LGL Used in the Building Trade

Through the centuries, stone masons developed their own terminology to distinguish and classify LGL, locally known in the building trade as "ġebla tal-franka", the Maltese translation for "freestone". Franka is a generic name. Grading LGL in terms of first- and second-quality lithotypes, a classification still widely used in the local quarrying industry, is rudimentary. Stone masons distinguish between franka and inferior quality, darker in color, less durable lithostratigraphical beds occurring within the LGL member [78]. Good quality LGL "rings" when hit by a mallet [79]. The inferior LGL is known as "sol" (or "soll", from the old Maltese word "saul" [48]), a limestone with "ħafna frak tal-ħġieġ" (literally translated as "many glass fragments") [79]. Such beds are present at approximately 12 m intervals in the good quality LGL [80]. Sol occurs in two varieties: "sol aħmar" (red sol) and "sol ikħal" (blue sol); the latter is also known as "ġebla l-kaħla" or "ħadra", which translates as "the blue stone" or "green". LGL has a specific blue-colored bed of sol ikħal, which is dark grey in color when freshly extracted but dries rapidly to pale grey when exposed [48]; it is suitable only for use in foundations and as fill [79]. Similarly colored lenticular patches are also present in this member. Based on a study of a site in Msida (UTM coordinates: 453212E, 3972483N) (Figure 1b), the mineralogy and geochemistry of these patches is quantitatively different from that of sol ikħal; their SiO_2 content is >10% whilst that of sol ikħal <10% [81]. The texture of the limestone forming these patches alternates from wackestone to mudstone to bioclastic wackestone. Petrographically, these variations are linked to process/es other than limestone texture. Whilst similar to sol ikħal, they differ

from sol aħmar, in which the micrite is often recrystallized to microspar [82]. For the scope of this paper, inferior LGL, also referred to as second-quality lithotype, refers to sol aħmar.

3. Materials and Methods

3.1. Sampling

The main sampling site is Tal-Warda softstone quarry at Qrendi (UTM coordinates: 451481E, 3966547N), officially known as Softstone Quarry No. 55 (Figure 1b). It is located adjacent to the Chapel of St Catherine. The site location, bordering with the locality of Mqabba, is plotted on the official aerial imagery, dated 1998, available at the Mapping Unit of the Planning Authority, Malta [83] (Figure 4). This open-pit mining site was selected because it was possible to correlate its position within the LGL. The top of the quarry is close to upper horizon of the LGL, that is, the base of the lower main phosphorite bed, a fact confirmed by infrastructure works which were being carried out on an adjacent road. The quarry was accessed via a ramp along its perimeter walls, so a visual inspection of its faces and the subsequent extraction of samples could be carried out with ease. The fault present in the upper part fell outside the sampling area. Based on a visual assessment, a number of beds were identified. The face of the quarry was classified in beds depending on varying bio-retexturing activity. Such classification—new to the local quarrying and building industry—was proposed as a way to explore the hypothesis that bioturbation is a reliable method to assess the quality of LGL. The relative position of the samples from the top of the quarry and their respective thickness were noted; thickness varied depending on the extent of burrowing activity in the host rock. In total, 16 samples from the host rock were analyzed; burrows were avoided. A summary of the sedimentological descriptions of the beds and of the hand specimens are given in Table 2. Sample locations were identified with the assistance of Dr Hugh Martyn Pedley. A lithostratigraphic column with respect to the general stratigraphy of the Maltese Islands is given in Figure 5.

Figure 4. Aerial imagery, dated 1998, of Tal-Warda quarry (outlined in red) and the Chapel of St Catherine (in red) [83]; for the location of site with respect to Malta, see Figure 1b.

Table 2. Visual description of limestone samples.

Bed No.	Thickness (m)	Limestone Quality	Sample ID	Position * (m)	Depth ** (m)	Description	
						Quarry Face	Hand Specimen
1	1.1	first	Q1_1 [1]	00.0	0.04	Burrows and occasional nodules are present.	Pale yellow in color; Burrows: 10% of the rock sample with diameter c. 3 mm; cream in color; sample had two dark yellow "iron stained" nodules.
2	0.2	first	Q1_2 [1]	01.1	1.2	Burrows dark brown and fine grained.	Pale yellow in color; Burrows: light brown in color.
3	1.3	first	Q1_3[1]	01.3	2.2	A few burrows with "iron stained" infill.	Pale to brown yellow; Burrows: with "iron stained" infill.
4	0.6	first		02.6			
5	1.7	second	Q1_4 [1]	03.2	3.8	Dark, heavily infilled, burrows with occasional red-brownish stains.	Cream colored, with shell fragments; Burrows: white infill with darker cream to yellow material surrounding them.
6	4.4	first	Q1_5	04.9	7.1	Occasional burrows with infill identical to host rock.	Pale to cream yellow in color.
7	1.2	second	Q1_6 [1]	09.3	10.2	Burrows progressively decreasing.	Pale yellow in color with shell fragments; Burrows: cream-colored infill.
8	1.5	first	Q1_7	10.5	11.3	Burrows rarely present; increase towards the top of the bed.	White in color; Burrows: diameter >18 mm, with pale brown infill.
9	3.0	second	Q1_8 [2]	12.0	13.1	Darker burrow infill decreasing towards the top of the bed.	White in color with some shell fragments; Burrows: brown and dark green/grey in color with occasional "iron stained" infill.
9	3.0	second	Q1_9 [1]	12.0	14.2	As Q1_8.	White in color with even whiter burrow infill.
10	4.3	first	Q1_10	15.0	18.0	No evidence of burrows.	Pale yellow in color with occasional shell fragments.
11	3.2	first	Q1_11 [2]	19.3	20.7	Though not heavily burrowed; quality is deteriorating upwards.	Pale yellow in color; Burrows: dark infill.
			Q1_12	19.3	21.7		
12	6.0	first	Q1_13	22.5	25.3	Sharp contact between host rock and burrows.	Pale yellow in color with shell fragments; Burrows: compact, cream yellow to dark green/grey infill.
12	6.0	first	Q1_14 [2]	22.5	28.1	Density of burrows increases up in the bed.	Pale yellow in color; Burrows: compact, cream yellow infill rich in shell fragments.
13	3.3	first	Q1_15	28.5	30.8	As per bed 12.	Cream colored with shell fragments; Burrows: two (10 and 12 mm in diameter) with cream-colored infill.
13	3.3	first	Q1_16	28.5	31.7	As per bed 12.	Cream-colored, weathered specimen rich in shell fragments; Burrows are present.

* Position of the upper side of the bed from quarry top; ** depth of extraction of sample; [1] reproduced in [41]; [2] reproduced in [84]; n.d.: not determined.

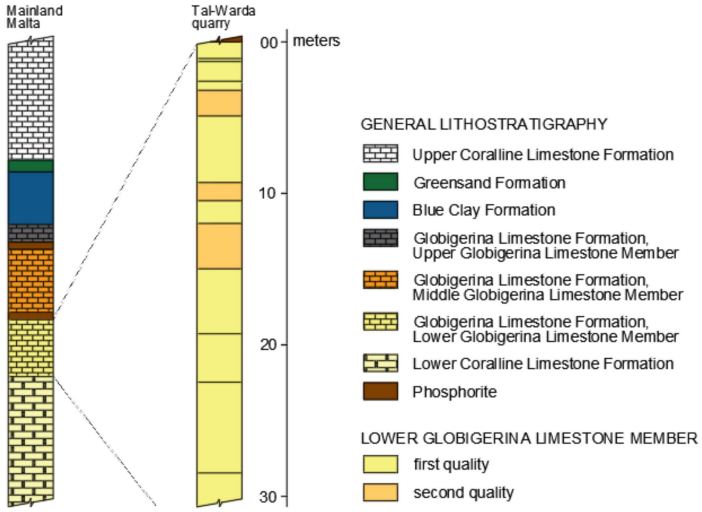

Figure 5. A lithostratigraphic column of Tal-Warda quarry with respect to the general stratigraphy of the Maltese Islands.

To comprehend what constitutes first-quality LGL, samples were taken from (i) the seventeenth-century Baroque Church of Santa Maria at Birkirkara (UTM coordinates: 451543E, 3972435N, Figure 1b), the subject of a recent publication [85] (Figure 6a) and (ii) Piccolo Fewda quarry, officially known as Softstone Quarry No. 32 (Figure 1b), in Mqabba (UTM coordinates: 447091E, 3584992N) which, at the time, was providing LGL for the restoration of the church [79,86]. Although in partial ruin until restoration works commenced in 1969, the original carvings on the main elevation of the church have weathered well, and the acanthus capitals are in optimal condition (Figure 6b). Thus, the limestone in which the church was erected arguably represents the best quality lithotype available at that time, which, according to tradition, was quarried from the limits of "Tal Balal" (UTM coordinates: 452223E, 3967432N). Old quarries in this locality were reclaimed for agrarian use, so the precise location of the site from which the original dimension stones were extracted is difficult to trace. Samples from the Piccolo Fewda quarry were collected with the assistance of the quarry owner Salvatore Bondin, a third-generation quarryman with over six decades of quarrying experience and a former President of the Softstone Quarries Association (of Malta).

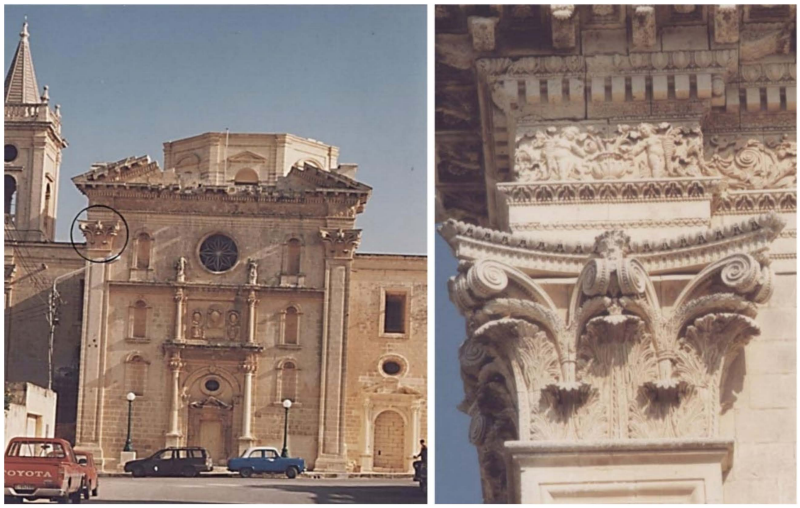

(**a**) (**b**)

Figure 6. Dated photo of: (**a**) The Church of Santa Maria, Birkirkara; (**b**) Detail circled in black in (**a**).

The terminology outlined in Section 2.4 was used when referring to the quarry at Mqabba. However, when referring to the quarry at Qrendi, the terms used refer to a visual criterion based on bioturbation—first-quality LGL has minimal burrowing, and burrowing increases with decreasing quality.

3.2. Characterization Techniques

The characterization of the samples was established through geochemical, mineralogical, textural and physico-mechanical analysis. Chemical analysis was determined through (i) loss-on-ignition (LOI), (ii) X-ray fluorescence (XRF) analysis and (iii) electron microprobe analysis. LOI—a measure of percentage loss in weight of an ignited sample due to the release of CO_2, water and other volatiles—was used to estimate the organic and carbonate content of sediments [87]. Standard-size polished thin sections coated with a thin carbon layer were used for the microprobe. To determine the bulk chemistry, an ARL 8420+ X-ray fluorescence spectrometer was used on pressed powder pellets [88]. To obtain an accurate elemental analysis of fossil fragments and grains, an electron probe microanalyzer was used. To establish qualitatively the mineralogy of the whole rock, the non-carbonate content and the clay fraction, a Philips PW1729 X-ray generator (XRD) was used. The mineralogy of the non-carbonate content was quantitatively established through acid insoluble residue (IR) in 10% HCl, whilst for the clay fraction, an oriented mount technique was used, since the d001 peaks are enhanced [89]. A glass mount and a piece of unused filter paper were analyzed as controls. Both XRF and X-ray diffraction analyses were undertaken at the former Department of Geology, now integrated in the School of Geography, Geology and the Environment, University of Leicester.

Optical and scanning electron microscopy (SEM) (for both rock specimens and insoluble residue) and mercury intrusion porosimetry (MIP) were used to obtain information on the texture. The cementing fabric, porosity and permeability were studied through thin section analysis; sections were impregnated with blue-dyed araldite for ease of reading the pore sizes and structure. To identify petrographically the distinction between first- and second-quality LGL as understood by the local quarrymen, samples Q from the Mqabba quarry and samples C from the Old Church were analyzed. They were re-examined by Professor Elena Koleva-Rekalova using a Zeiss Axioskop 40 transmitted light microscope, which was equipped with a digital camera for taking microphotographs in both plane-polarized and cross-polarized light [90]. The classification of the limestone was performed according to Dunham's scheme [91]. Texture, cement fabric and pores, as well as the non-carbonate fraction, were analyzed using a Hitachi S-520 scanning electron microscope equipped with an energy dispersive analyzer [92,93]. To avoid contamination, fragments (measuring circa $5 \times 5 \times 5$ mm) were freshly cut from the sample retained following thin section preparation. To ensure good quality imaging, these fragments were handled to evade contact with skin oil which might out-gas in the SEM vacuum system. Furthermore, a film of conductive paint was applied to ensure electrical contact between the fragment and the stub and, to ensure good quality imaging, a thin gold coating was applied. MIP was used to establish the volumes and radii of pores within the fabric [94,95]. A Quantachrome SP-33B mercury intrusion porosimeter was used. All analyses were undertaken at the University of Leicester except for MIP, which was carried out at the Department of Civil Engineering of the Faculty of Architecture and Civil Engineering, the forerunner of the Faculty for the Built Environment, of the University of Malta, Msida, Malta.

To evaluate the physico-mechanical properties, the following testing regimes were used: (i) apparent density, (ii) compressive strength (CS), using the Avery-Denison model, (iii) ultrasonic pulse velocity (UPV), using the PUNDIT model, and (iv) color, using (EEL) Abridged Reflectance Spectrometer model. For regimes (i) to (iii), tests were undertaken on oven-dried (temperature $105+/-5$ °C) and saturated (fully submerged for 24 h) samples. With the exception of color analysis, which was undertaken at the Department of Geology, University of Leicester, all other testing regimes were carried out at the Department of

Civil Engineering, University of Malta. This decision was undertaken to cut down on the bulk handling of the large samples required for the petrophysical testing regimes.

4. Results

4.1. Geochemistry

The XRF analyses for major oxides and the LOI are given in Table 3. LOI was <44%, the theoretical value for pure $CaCO_3$. Samples Q1_4 and Q1_6, identified in the field as second-quality LGL (Table 2), have low $CaCO_3$, whilst samples Q1_8 and Q1_9 have a $CaCO_3$ content comparable to first-quality lithotype. A lower $CaCO_3$ content is present in Q1_15. Burrow infills at the stratigraphic level from which Q1_8 was extracted had a similar $CaCO_3$ content to first quality, while similar infills at the lithostratigraphic beds from which Q1_11 and Q1_14 were extracted had a similar $CaCO_3$ content to second-quality lithotype [84], which indicates that burrowing activity introduced material different from the host rock.

Table 3. LOI and chemical composition (%).

Sample ID	LOI	X-ray Fluorescence Analysis									
		CaO	SiO_2	Al_2O_3	MgO	Fe_2O_3	K_2O	P_2O_5	TiO_2	Na_2O	MnO
Q1_1 [1]	41.37	49.389	07.954	01.288	01.176	00.739	00.425	00.220	00.184	00.037	00.032
Q1_2 [1]	41.72	49.668	06.767	01.062	01.142	00.595	00.356	00.211	00.151	00.042	00.033
Q1_3 [1]	42.24	50.044	05.516	00.806	01.113	00.498	00.278	00.204	00.122	00.025	00.035
Q1_4 [1]	40.43	48.165	09.695	01.388	01.140	01.038	00.512	00.300	00.221	00.057	00.036
Q1_5	41.49	49.245	07.021	00.856	00.988	00.652	00.360	00.243	00.148	00.062	00.034
Q1_6 [1]	39.43	46.651	11.985	01.615	01.157	00.978	00.634	00.258	00.258	00.090	00.033
Q1_7	41.44	48.778	07.218	00.919	01.189	00.742	00.370	00.285	00.128	00.066	00.034
Q1_8 [2]	41.75	49.577	06.506	00.838	01.173	00.822	00.369	00.707	00.117	00.055	00.035
Q1_9 [1]	42.18	49.671	06.329	00.856	01.137	00.649	00.332	00.310	00.107	00.058	00.034
Q1_10	42.60	50.088	04.847	00.584	00.989	00.450	00.224	00.218	00.083	00.065	00.032
Q1_11 [2]	42.81	50.222	04.272	00.434	00.719	00.317	00.185	00.186	00.070	00.071	00.036
Q1_12	42.83	49.619	04.054	00.398	00.994	00.420	00.171	00.546	00.067	00.084	00.035
Q1_13	42.57	49.772	04.452	00.434	01.116	00.367	00.194	00.576	00.075	00.073	00.034
Q1_14 [2]	42.01	48.789	05.094	00.513	01.172	00.633	00.251	01.080	00.084	00.141	00.036
Q1_15	41.27	48.545	06.801	00.726	01.180	00.781	00.304	01.121	00.124	00.114	00.037
Q1_16	41.87	49.435	06.109	00.651	01.133	00.656	00.281	00.952	00.097	00.037	00.036

[1] Reproduced in [41]; [2] reproduced in [84].

The main non-carbonate fraction is SiO_2 (Figure 7); its presence is inversely proportional to the $CaCO_3$ content. The variation in Al_2O_3, Fe_2O_3, K_2O and TiO_2, although less pronounced, is similar to SiO_2 (Figure 8). Second-quality LGL is characterized by higher content of these oxides; the variation between beds 9 and 15 is gradual. The presence of MgO, which does not correlate with any noted variation in the quality of LGL, may be due to change in allochem mineralogy [96]. Na_2O and MnO are present in traces. Electron probe analysis of the host rock and burrow infills showed alteration in the composition due to iron oxide and glauconite breakdown.

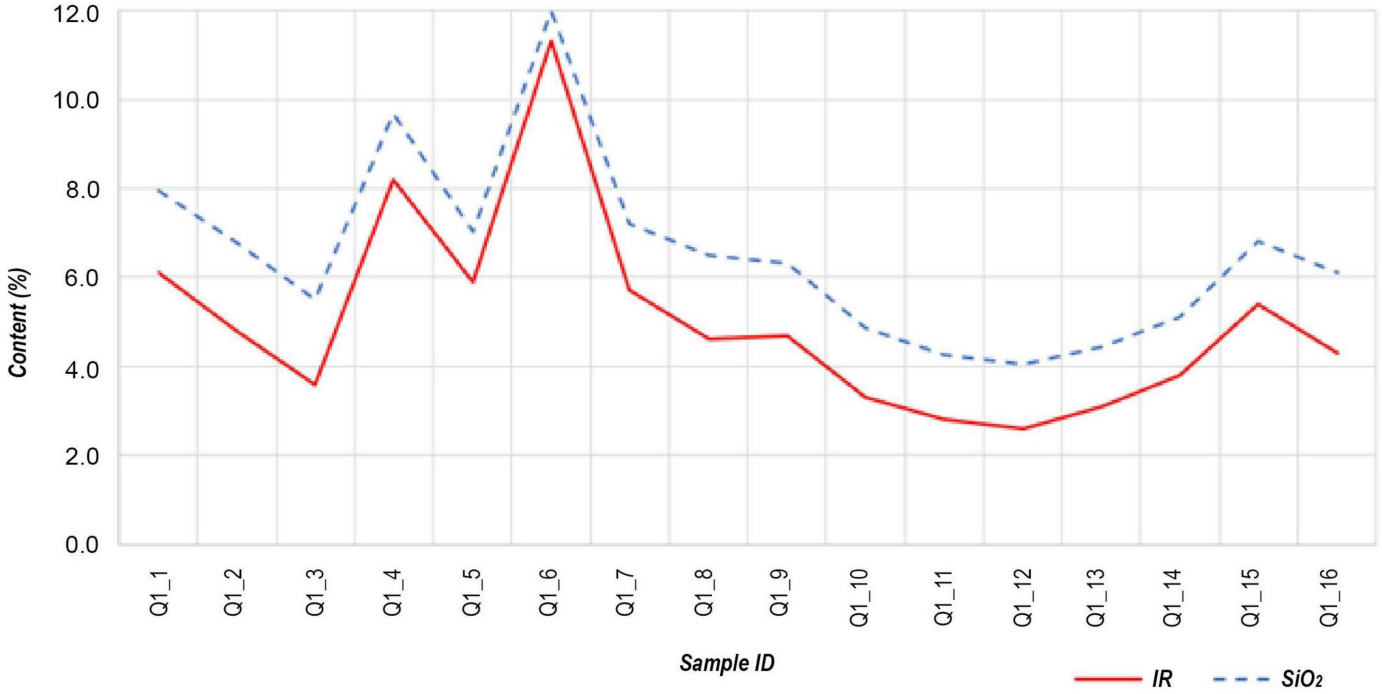

Figure 7. Variations in IR and SiO_2.

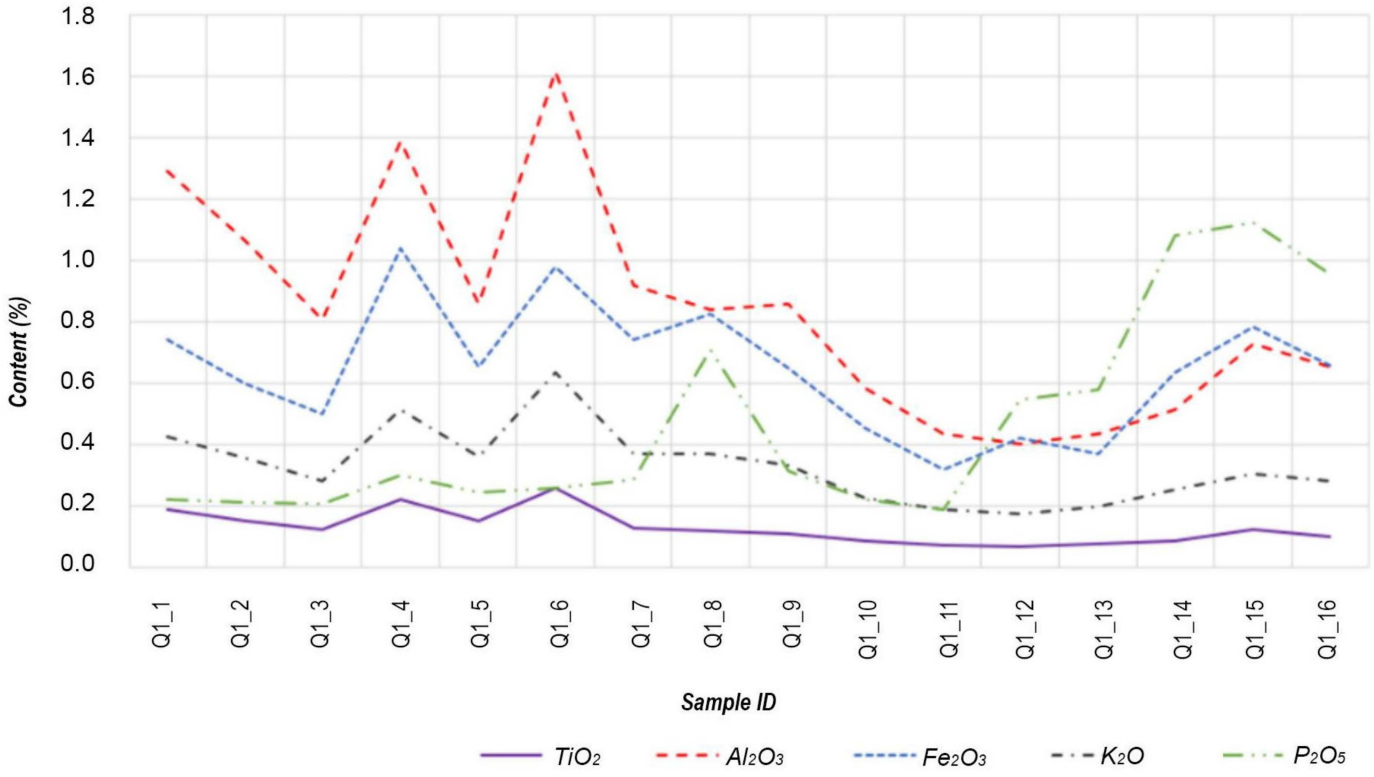

Figure 8. Variations in TiO_2, Al_2O_3, Fe_2O_3, K_2O and P_2O_5.

Analysis of samples from Mqabba quarry and church converge to similar results. $CaCO_3$ content decreases progressively as the quality of the LGL decreases [85]. The principal non-carbonate oxides—SiO_2, Al_2O_3, Fe_2O_3 and K_2O—are minimally present in the first-quality LGL.

Sol ikħal has a lower $CaCO_3$ content than sol aħmar which, in turn, has a lower $CaCO_3$ content than first-quality LGL [81,85]. Based on first-quality LGL from both sites, LGL with an IR content of $\geq$5% is of inferior quality.

XRF is often used to verify the XRD data and vice versa. Analysis of the chemical composition of geological samples using the semi-quantitative analysis method can be used to determine elemental composition of rocks. The data on oxides obtained via current methods are useful for geochemical characterizations of the limestone and for corresponding interpretations. These oxides can be attributed to quartz, clays, K-feldspar, muscovite and some iron oxide/s. These data are not useful, however, for determining the mineral composition. For example, it is not possible to estimate how much SiO_2 comes from quartz, kaolinite, etc.

4.2. Mineralogy

The mineralogical analysis, including the fraction of the IR, is given in Table 4. The various types of XRD traces are given in Figure 9.

Table 4. IR and X-ray diffraction analysis: summary of identified minerals.

Sample ID	IR (%)	X-ray Diffraction Analysis [1]															
		Whole Rock	IR										Clay Fraction				
		cal	qtz	qtz	Kfs	ms	kln	ill	sme	gp	al	rt	kln	ill	sme	qtz	Kfs
Q1_1 [1]	06.1	x	x	x	x	x	x						n.d.	n.d.	n.d.	n.d.	n.d.
Q1_2 [1]	04.8	x		x	x		x	x					x	x	x	x	x
Q1_3 [1]	03.6	x	x	x	x	x	x						n.d.	n.d.	n.d.	n.d.	n.d.
Q1_4 [1]	08.2	x	x	x	x	x							x	x	x	x	x
Q1_5	05.9	x	x	x	x	x							n.d.	n.d.	n.d.	n.d.	n.d.
Q1_6 [1]	11.3	x	x	x	x	x							n.d.	n.d.	n.d.	n.d.	n.d.
Q1_7	05.7	x	x	x	x	x							n.d.	n.d.	n.d.	n.d.	n.d.
Q1_8 [2]	04.6	x	x	x	x	x	x						n.d.	n.d.	n.d.	n.d.	n.d.
Q1_9 [1]	04.7	x	x	x	x	x							n.d.	n.d.	n.d.	n.d.	n.d.
Q1_10	03.3	x	x	x	x	x	x						n.d.	n.d.	n.d.	n.d.	n.d.
Q1_11 [2]	02.8	x		x	x				x		x		x	x	x	x	x
Q1_12	02.6	x		x	x			x	x	x			n.d.	n.d.	n.d.	n.d.	n.d.
Q1_13	03.1	x	x	x	x	x		x					x	x	x	x	x
Q1_14 [2]	03.8	x	x	x	x	x						x	n.d.	n.d.	n.d.	n.d.	n.d.
Q1_15	05.4	x	x	x	x	x		x					n.d.	n.d.	n.d.	n.d.	n.d.
Q1_16	04.3	x	x	x	x	x							x	x	x	x	x

[1] Reproduced in [41]; [2] reproduced in [84]; x: mineral is present; n.d.: not determined.

Further to calcite (cal), quartz (qtz) was identified in the whole-rock analysis in all samples except for a few of the first-quality samples (Figure 9a). Analysis of the insoluble residue indicates that these samples are characterized by the absence of muscovite (ms); quartz and K-feldspar (Kfs) are present in all samples (Figure 9b,c). Kaolinite (kln), illite (ill) and smectite (sme) are sometimes present. Burrows present in the beds from which samples Q1_8 and Q1_11 were extracted contain goethite [84]. Inferior-quality LGL from Mqabba quarry contains geothite. This mineral—typically formed under oxidizing conditions and includes material frequently grouped as limonite—occurs as a weathering product of iron bearing minerals such as pyrite. Gypsum (gp), albite (al) and rutile (rt) are occasional. Kaolinite, illite, smectite, quartz and K-feldspar make up the mineralogy of the clay fraction (Figure 9d–f). Second-quality beds have higher non-carbonate content. Although identified as being first quality, sample Q1_15 has an IR content similar to second-quality lithotype. The variation in the non-carbonate content from samples Q1_9 to Q1_15 is gradual.

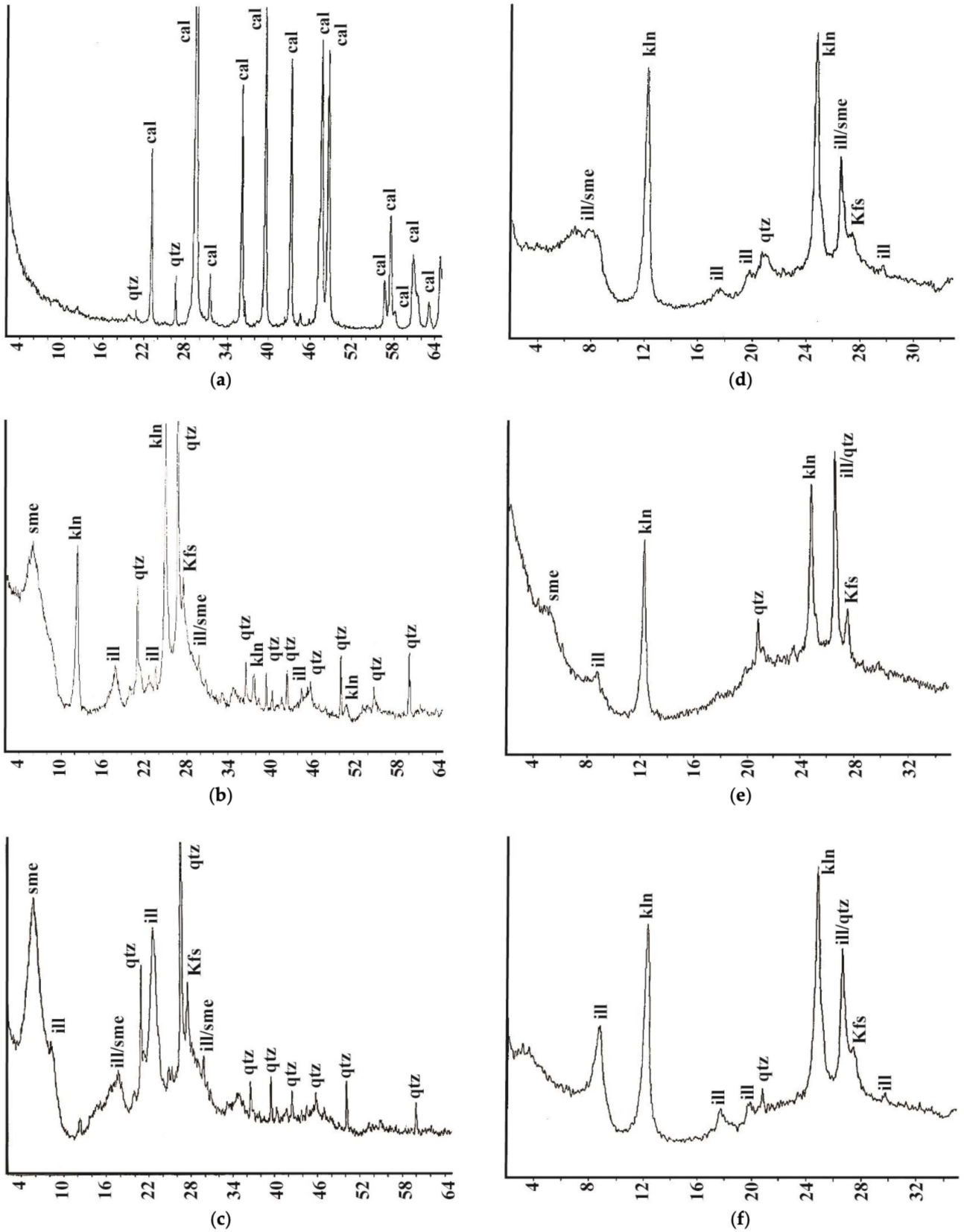

Figure 9. XRD trace patterns of 2Theta (°) (x-axis) versus intensity (a.u.) (y-axis): (**a**) whole rock for samples Q1_1 to Q1_16; (**b**) insoluble residue for samples Q1_1 to Q1_10; (**c**) insoluble residue for samples Q1_11 to Q1_16; and clay fraction for selected samples Q1_2 and Q1_4, (**d**) air-dried; (**e**) glycolated; (**f**) heated.

4.3. Texture

4.3.1. Optical Microscopy

Samples analyzed are of intra- and inter-particle porosity type, the former more frequent than the latter. They consist of fine-grained Globigerina-bioclastic wackestone, which alternates with Globigerina-bioclastic packstone until the latter becomes the main fabric, from bed 11 and lower. The sediment is comprised of planktonic and benthonic foraminifera; rare echinoid fragments are also present. Undamaged microfossils have unfilled chambers. Allochems are cemented by fine-grained sparry calcite; they imperfectly fill the inter-particle voids. Porosity along grain boundaries is predominant in the host rock compared to the burrow infill. Quartz grains—elongated or rounded and dispersed through the matrix—glauconite, and some iron oxide/s are also present. Staining due to breakdown of iron-rich minerals is present.

The petrographical characteristics of the C and Q samples are given in Table 5. Samples C1 and C2 are from the undeteriorated and deteriorated surface, respectively. Sample Q1 is first-quality LGL, Q2 is identical to Q1 but seasoned for 12 years, and Q3 is second-quality LGL. Irrespective of the quality of the LGL, all samples are Globigerina wackestone. In Q1, the micrite is darker in color; only in some places it is recrystallized to microspar and spar. Small planktonic Globigerina foraminifera occur. Single and strongly altered benthic foraminifera are presented. The bioclasts of echinoids and bivalves are very rare, altered and difficult to discern. In Q2, the micrite in the matrix is commonly recrystallized to microspar. Small planktonic Globigerina foraminifera predominate. Single and strongly altered benthic foraminifera are present. The bioclasts of echinoids are rare, with sizes less than 1.0 mm; some glauconite grains are visible. In Q3, the micrite is commonly recrystallized to microspar. It is preserved only in some places that resemble micrite intraclasts. Planktonic Globigerina foraminifera occur. Rare bioclasts and single benthic foraminifera are present. Only one bivalve fragment, 1.2 × 0.03 mm in size, is present; glauconite grains are sporadic.

Table 5. Petrographical characteristics (%).

Characteristics	Sample ID [1]				
	Old Church, Birkirkara		Mqabba Quarry		
	C1	C2	Q1	Q2	Q3
Matrix	80	75	80	70	65
Allochems	20	25	20	30	35 [2]
Terrigenous components	single; sizes < 0.1 mm	sparodic; sizes < 0.08 mm	rare	rare	rare
Classification	wackestone	wackestone	wackestone	wackestone	wackestone

[1] The analyses of these samples are contained in [85]; [2] there is a typo error in [85].

Unlike the Q samples, in which terrigenous components are rare, they are sporadic in the C samples. In C1, the micrite in the matrix is preserved only in some places (Figure 10). It is frequently recrystallized to microspar and rarely to spar. In the more recrystallized areas, more pores are observed. In some places the recrystallization obliterates the primary texture of the limestone. Small planktonic Globigerina foraminifera dominate and most often their chambers represent pores. Bioclasts are very rare and predominantly they are represented by echinoids, whose sizes do not exceed 0.5 mm. There are sporadic benthic foraminifera. In C2, the micrite matrix displays darker coloration (Figure 11); micrite is frequently recrystallized to microspar and in these places the pores are of an insignificant quantity. Small planktonic Globigerina foraminifera predominate. Commonly their chambers are empty. Bioclasts are very rare, and their sizes are less than 0.5 mm. Single echinoid fragments are with syntaxial overgrowths. One bioclast (0.45 × 0.3 mm) is silicified.

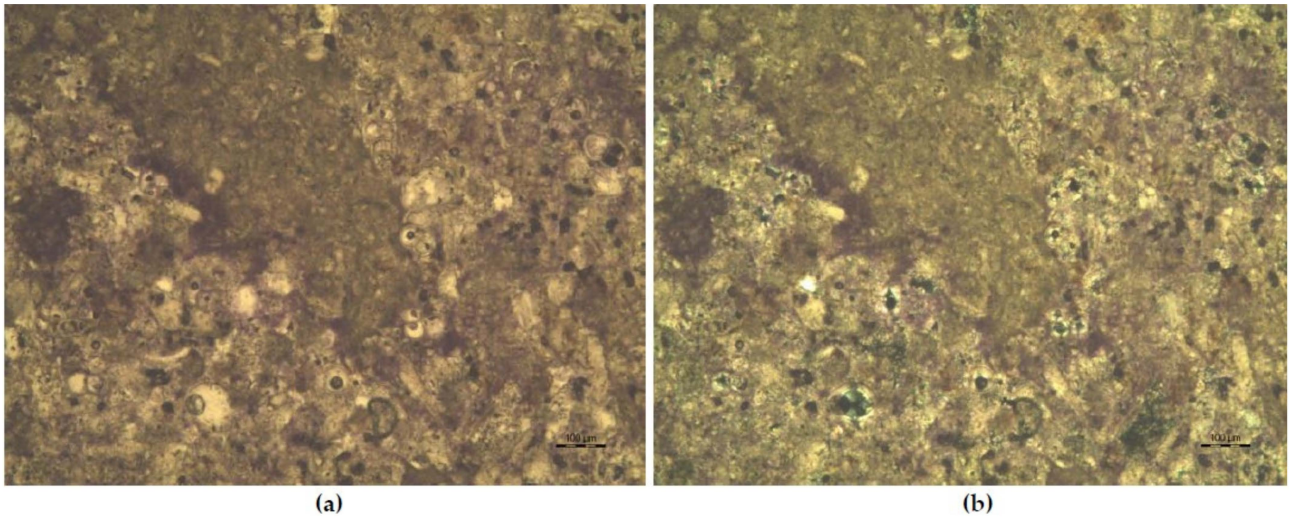

Figure 10. Sample C1: (**a**) plane-polarized light: micrite is recrystallized to microspar and containing planktonic Globigerina and benthic foraminifera, in the central part the micrite is preserved and looks like as micrite intraclast; (**b**) cross-polarized light: same view as (**a**), intraparticle porosity.

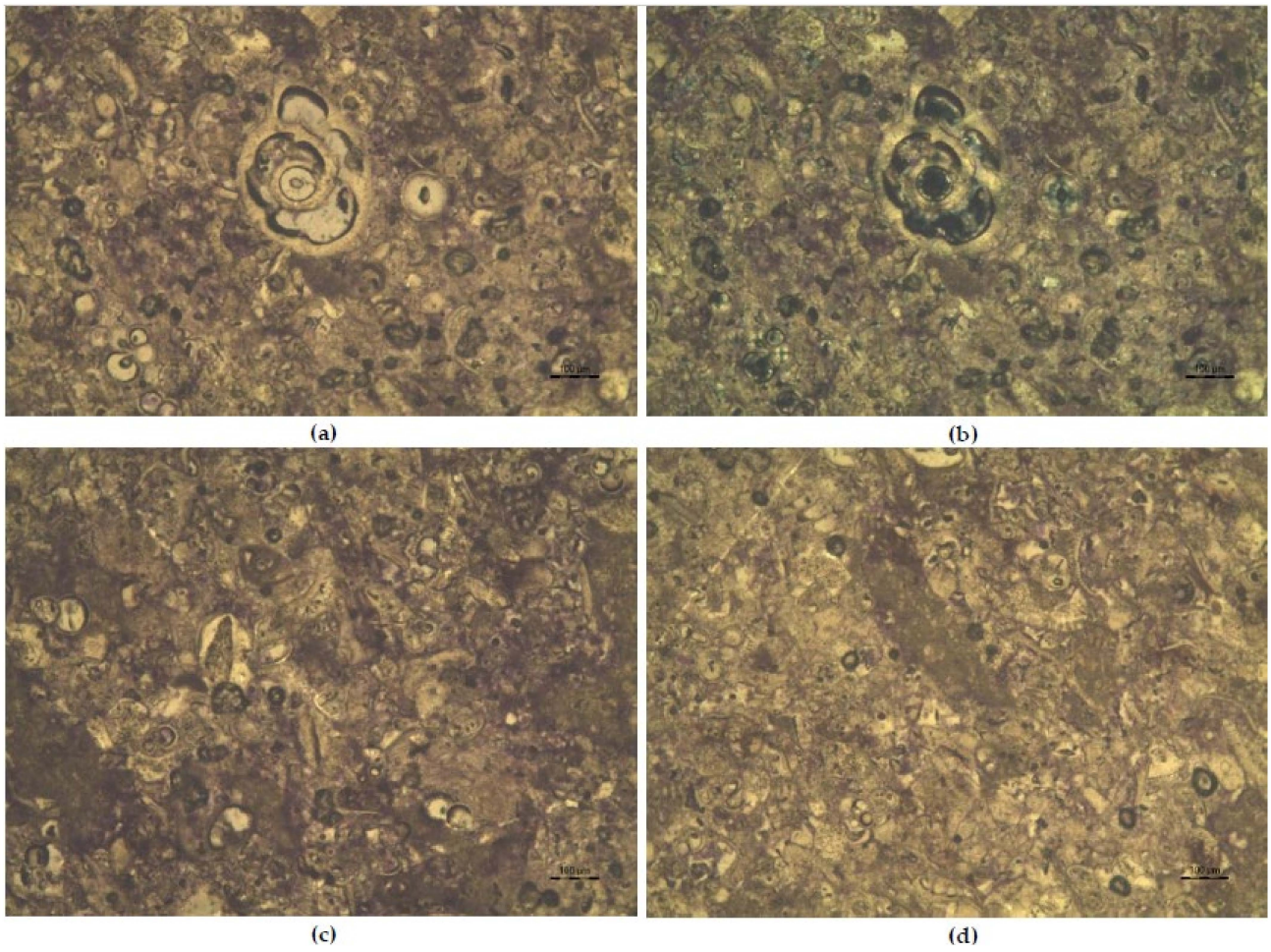

Figure 11. Sample C2: (**a**) plane-polarized light: parallel nicols, micrite matrix with planktonic Globigerina foraminifera and rare bioclasts; (**b**) cross-polarized light: same view as (**a**), inter-particle porosity; (**c**) plane-polarized light: micrite matrix with planktonic Globigerina foraminifera and bioclasts, in the central part an echinoid fragment with syntaxial overgrowth; (**d**) plane-polarized light: micrite is recrystallized to microspar and containing planktonic Globigerina foraminifers, single benthic foraminifera and bioclasts; in the central part the micrite is preserved and looks like a micrite intraclast.

4.3.2. Scanning Electron Microscopy and Porosimetry

Three samples were analyzed through SEM: Q1_1 and Q1_6, first- and second-quality LGL, respectively, and a sample from the church. Microphotographs are given in Figure 12. The pore structure, the physico-mechanical interlocking and the fine-grained cement are shown in Figure 12a,b; fine-grained sparry calcite, which fills the inter-particle voids, cements most allochems. Although more samples are required for robust conclusive evidence, it is evident that the post-depositional, compact, low permeability LGL might have originally been very porous. The passage of water through the matrix encouraged the growth of the post-depositional interlocking calcite crystal fabric present in the church sample (Figure 12b). Such interlocking crystals provide a physico-mechanical bond which produces a more durable building stone.

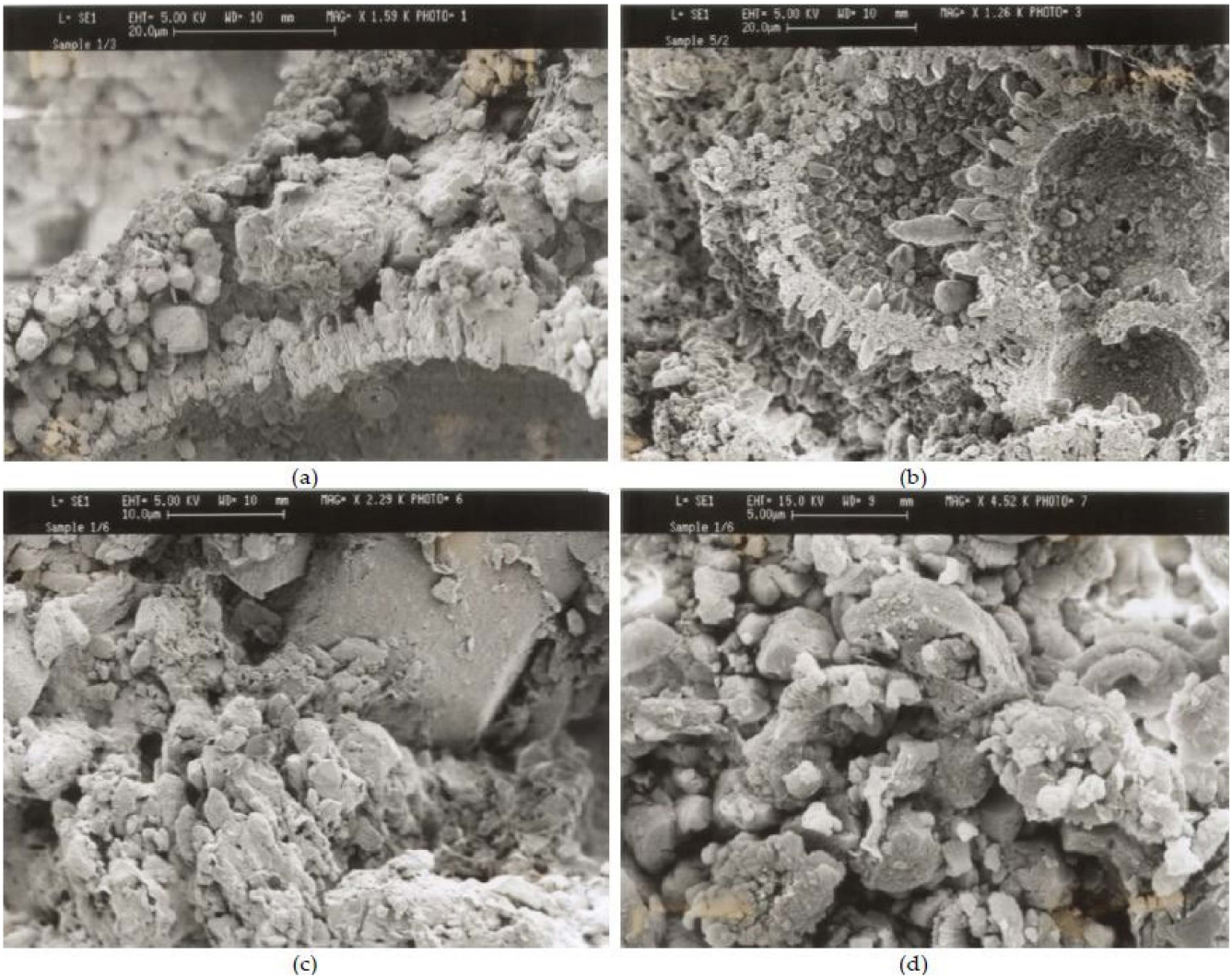

Figure 12. SEM images illustrating the pore structure, the physico-mechanical interlocking and the fine-grained sparry calcite cement of samples from: (**a**) the first-quality bed within Tal-Warda quarry; (**b**) the Church of Santa Maria, Birkirkara; (**c**) the second-quality bed within Tal-Warda quarry; (**d**) micrite matrix in the second-quality bed within Tal-Warda quarry.

Table 6 summarizes the interpolated intruded volume for each sample analyzed through MIP. When comparing the results from the Qrendi quarry with those from the Mqabba quarry and the church samples, variations in the distribution of the pores can be observed, which is indicative of petrographical differences arising from the provenance of the limestone [85]. In the latter two sites, the volume of pores is higher in first-quality LGL. A similar correlation, although less defined, is present at Tal-Warda quarry.

Table 6. Interpolated mercury intrusion pore radius.

Sample ID	Total Volume	Volume in Pores (cm^3/g)		
		Pore Radius >40,000Å	Pore Radius 40–40,000Å	Pore Radius <40Å
Q1_2 [1]	0.1097	0.0018	0.1071	0.0008
Q1_4 [1]	0.0923	0.0001	0.0898	0.0024
Q1_6 [1]	0.0893	0.0068	0.0821	0.0004
Q1_9 [1]	0.1092	0.0011	0.1072	0.0009
Q1_11	0.0600	0.0001	0.0593	0.0006
Q1_13	0.0917	0.0112	0.0803	0.0002
Q1_14	0.1084	0.0112	0.0960	0.0012

[1] Reproduced in [41].

4.4. Petrophysical Properties

The relative density varies: lower quality LGL has higher density, an indication that particle porosity is higher in better-quality LGL (Table 7). Subject to a constant loading rate set at 0.15 N/mm^2, the CS of 100 × 100 × 100 mm samples varies between 15.6–30.2 N/mm^2 for dry states and 8.3–17.4 N/mm^2 for saturated states; this is within the range stated in the national structural handbook [97]. The host rock of sample Q_11 is first quality, but the presence of burrows reduces its quality. Inferior LGL characteristically has higher mean dry compressive strength (f_k) and lower porosity. According to the Centre Technique de Matériaux Naturels de Construction [98], LGL is definitely not a hard stone ($f_k > 40$ N/mm^2) [99]; some lithostratigraphic beds qualify as a compact ($10 \leq f_k \leq 40$ N/mm^2) rather than as a soft stone ($f_k < 10$ N/mm^2). No significant variation in CS between the two lithotypes is present. An anomaly is present in sample Q1_11, a first-quality LGL with visually pronounced dark burrow infill (Table 2). UPV values follow a similar pattern, both perpendicular and parallel to the bedding plane. Correlation is present between UC and UPV values, a result in line with Vasanelli et al. [100]. Applying the classification for UPV [101], velocities in the range of 2.5–3.5 km/s were considered low, and wet samples yielded lower values [100].

Table 7. Petrophysical analysis.

Sample ID	Apparent Density (kg/m^3)		CS (N/mm^2)		UPV (km/s)	
	Oven Dried	Saturated	Oven Dried	Saturated	Perpendicular	Parallel
Q1_2 [1]	1778	2016	30.18	15.42	3.06	2.99
Q1_4 [1]	1844	2068	28.83	12.89	2.91	2.97
Q1_6 [1]	1844	2067	25.30	15.26	2.98	2.99
Q1_9 [1]	1719	1954	21.82	15.09	2.91	2.86
Q1_11	1717	1949	15.58	08.27	2.69	2.71
Q1_13	1784	1975	27.88	17.43	3.22	3.11
Q1_14	1787	1999	22.54	16.95	3.07	2.94

[1] Reproduced in [41].

For all samples, the hue was yellow as the color wavelength varied between 580 and 582 nm. (Table 8). Variations were present in wavelength, purity (or chroma) and brightness (or value, tone). A possible correlation between density and color—a third-order polynomial—was found: the darker the color, the higher the density.

Table 8. Color measurements.

Sample ID	Wavelength (nm)	Purity (%)	Brightness (%)	Filter Value			L *	a **	b ***	Eab #	Eab *##
				Red (x)	Green (y)	Blue (z)					
Q1_1	581	75	70.5	72.5	75.3	61.2	89.54	−5.70	12.14	137.85	3.57
Q1_2	581	75	71.5	73.9	76.5	63.3	90.10	−5.24	11.18	138.06	3.36
Q1_3	582	75	71.7	74.3	76.8	63.8	90.24	−5.02	10.97	138.02	3.40
Q1_4	580	75	69.1	70.4	73.8	57.0	88.84	−7.04	14.90	137.20	4.22
Q1_5	580	75	72.7	75.0	77.7	63.3	90.65	−5.38	12.13	137.53	3.89
Q1_6	580	75	69.8	71.6	74.6	59.5	89.22	−6.16	13.16	137.57	3.85
Q1_7	582	75	71.3	73.6	76.4	62.1	90.05	−5.65	12.19	137.73	3.69
Q1_8	582	75	71.4	73.6	76.5	62.2	90.10	−5.85	12.18	137.89	3.53
Q1_9	582	75	73.2	75.6	78.2	65.1	90.88	−5.16	10.91	138.12	3.30
Q1_10	582	73	75.3	78.9	80.6	69.1	91.96	−3.29	09.30	137.70	3.72
Q1_11	582	73	77.6	81.1	83.0	72.0	93.02	−3.61	08.69	138.28	3.14
Q1_12	582	75	74.4	77.2	79.6	67.1	91.51	−4.70	10.25	138.16	3.26
Q1_13	582	75	74.2	77.4	79.3	67.8	91.38	−3.72	09.41	137.98	3.44
Q1_14	582	75	70.4	72.4	75.6	60.6	89.68	−6.51	12.94	137.95	3.47
Q1_15	580	75	69.3	71.2	74.2	58.8	89.03	−6.18	13.50	137.39	4.03
Q1_16	580	75	71.2	73.4	75.8	61.0	89.78	−4.86	12.73	136.81	4.61

* $L = 116[(y/100)^{1/3}] - 16$; ** $a = 500[(x/100)^{1/3} - (y/100)^{1/3}]$; *** $b = 200[(y/100)^{1/3} - (z/100)^{1/3}]$; # $Eab = [(L - 100)^2 + (a - 100)^2 + (b - 100)^2]^{1/2}$; ## Eab* = (141.42 − Eab).

5. Discussion

5.1. Lithology

Composed of skeletal and shell fragments, variations in non-carbonate content in the lithostratigraphy of LGL may be due to the Miocene environmental changes that took place during its formation or due to changes in the source area of the sediments. Sediment input appears to have changed at the same time that small quantities of non-carbonate minerals intruded into areas where carbonates were being deposited.

According to the widely used Institute of Geological Sciences classification of limestone purity based on $CaCO_3$ content [102], the LGL is of medium (93.5% < $CaCO_3$ < 97.0%) to high (97.0% < $CaCO_3$ < 98.5%) purity, and purity increases with quality. Only some beds of the first-quality lithotype are of high purity. Principal limestone characteristics are imperative for effective damage diagnostics [103,104].

Until the completion of Bianco [40], the quality criteria used to differentiate between the two LGL lithotypes were based on consideration of CS, porosity, "ringing tone" and "glass fragments". The best-quality LGL does indeed have marked lithophonic characteristics when hit by a mallet, whilst inferior-quality stone is richer in quartz splinters.

The mineralogy determines the properties of LGL to a large extent, whilst the pore size controls strength, durability and the movement of moisture. Durability and CS are not interchangeable, an error often made by quarrymen [41,85]. Whilst it is indicative of the stone's quality, the durability of both lithotypes depends not only on the strength of the constituents making up the fabric but on the physico-mechanical interlocking and the sparry calcite cement where the grains come into contact. Although quartz, the main non-carbonate mineral, is considerably hard, it is cemented with the softer calcite, thus the overall hardness and strength are weak. The cement bonding the minerals and other organic fragments is a controlling factor in strength and durability. This cement also influences the tensile strength of the fabric. Generally, brittle fractures start at grain boundaries; the grains will loosen and become detached as stresses increase until tension is released on failure. The failure path along both LGL lithotypes is illustrative of the weakest path along which stresses are transmitted. Failure along this path requires minimal energy.

5.2. Compressive Strength

Compressive strength (CS) is an indicator of the strength of LGL but is not indicative of durability. Both factors depend on the kind of cement and the degree of cementation. In the inferior lithotype (Figure 12c,d), an occasional film of precipitated calcite crystals coats the individual fragments and cements the fragments. CS is provided by well-distributed

calcite cement. No cement is present in the interstices between the grains. The first-quality LGL supports more extensive re-crystallization.

The non-carbonate content includes minerals of varying coefficients of thermal expansion. Differential expansion of these minerals generates stress at both inter- and intra-particle pores and causes the breakdown of the cementing fabric and the development of micro-cracks within the sediment. It is important that stone cutting and dressing should be done in such a way that the dimension stone produced is free from micro-cracking, as damage can be induced by bad workmanship. Low CS values may arise from micro-cracks caused by using the mallet too heavily when dressing the stone or by mishandling the dimension stone during building works.

5.3. Porosity

Given that the porosity along grain boundaries is predominant, the type and percentage of pores are key to both the mechanical behavior and durability of LGL. The results seem to demonstrate that the grain boundaries are an effective pathway enabling the fluid to penetrate the limestone fabric faster compared to other porosity structures. The matrix to allochems ratio decreases with decreasing quality. The micrite in the matrix is commonly recrystallized to microspar, which obliterates the primary texture of the LGL; it is preserved only in some places that resemble micrite intraclasts. Overall porosity and pore space distribution depend on the heterogeneity of the formation. Generally, for carbonates, the depositional porosity varies from 40% to 70% when uncemented. After lithification it may vary from 5% to 15% [105]. The porosity of first quality LGL is 39+/−1% [106], a value endorsed by Morris [107]. Both LGL lithotypes predominately contain pores with radii ranging from 40 to 40,000 Å, although the inferior lithotype is less porous. The lower the volume of pores, the lower the "life-span" of the LGL, and the more likely it is to have higher thermal conductivity.

The effect of carbonic acid, an important solvent agent in limestone, increases with increasing micro porosity. The dissolving action is prolonged by capillary action which, in turn, ensures that water is retained in the micropores for a longer duration. Variation in effective porosity in both lithotypes requires further investigation.

SEM imagery shows euhedral interlocking calcite crystals, which suggests that the first-quality LGL might originally have been very porous. Porosity is modified by post-depositional processes. The passage of water through the matrix encouraged the growth of the post-depositional dog-tooth calcite crystal fabric present in the first quality LGL (Figure 12a,b). Calcite mud in the second-quality LGL (Figure 12c,d) prevents the flow of water through the fabric, thus it lacks the euhedral dog-tooth interlocking calcite crystals present in the first-quality lithotype. These crystals provide a bonding agent which produces a more durable building stone. Therefore, the diagenetic history of the limestone is important in its eventual quality.

5.4. Weathering

The weathering and durability properties of LGL have long been a topic of interest, with references found throughout history [4,108,109]. Systematic research into the limestones of Malta, including LGL, was conducted by the Building Research Station [110–112], and models describing the weathering and decay of the Globigerina Limestone have been published notably by Fitzner et al. [113] and Sandrolini et al. [114]. Weathering of LGL is also a theme within an ongoing project run by the Geological Institute of the Bulgarian Academy of Sciences [115].

Limestone matrix varies with the environment of deposition and the subsequent lithostratigraphic history. Chemical processes of weathering are aided by physical breakdown, which increases the surface area of fragment surfaces, thus providing easier access to oxygen and moisture which further perpetuate and accelerate chemical breakdown. The presence of oxygen leads to oxidation, while the presence of moisture leads to solution or hydration. With the advent of industrialization, the rate of decay of limestone increased

dramatically. Photographs taken in the mid-nineteenth century indicate that the fortifications along the Valletta seafront started to deteriorate at a high rate following the advent of the first coal-operated ships frequenting the harbor [116]. This may have been due to sulfur emissions in the air causing acid attack to the limestone.

Porosity is related to the weathering resistance of limestone. Pore structure has a bearing on weathering [117]: (i) the shape, size and nature of pores, (ii) how they are connected, and (iii) the degree of micro-porosity (pores < 0.025 mm) are important parameters. The importance of these three factors is illustrated by photographs of buildings utilizing CL. The weathered limestone of the bastions facing Marsamxett Harbor has large voids [29]. The larger the weathered voids, the easier it is for water to move in and out of the fabric without causing major damage, even though the surface area on which weathering can occur is increased.

Results from XRF (Table 3), and IR and XRD (Table 4) analysis converge to show that non-carbonate impurities are lower in first-quality LGL. The principal non-carbonate components are attributed to quartz, clays, feldspars, muscovite and some iron oxide mineral/s. Quartz and mica are resistant to weathering. Feldspars weather slowly to kaolinite and illite. Illite and smectite are structurally related to micas; most of the interlayer water of smectite is lost on heating to 335 °C. Illite is a clay mica similar to kaolinite; it differs from muscovite in that it has less potassium and more silica [118] and may be formed during diagenesis by alteration of other clay species. Illite may result from post-depositional weathering of muscovite and silicates, in particular feldspars. Kaolinite absorbs water without swelling; it is sometimes a byproduct of the weathering of feldspars and other silicates. Smectite is also an end product of weathering; unlike kaolinite, it is a swelling clay. These mineralogical changes are more significant in the inferior lithotype. Ferric compounds present in thin sections may be due to weathering of glauconite. Goethite and limonite are weathering end products. The latter may be considered as goethite plus amorphous ferric hydroxide.

Alveolar weathering characterizes LGL; this is due to (i) selective intra-burrow cementation and (ii) preferential erosion of the adjacent weakly cemented sediment. The "marki tas-swaba" (literally "finger marks) [79] are the profiles of preferential weathering in areas where burrows are present. Salt crystallization, long identified as the primary cause of LGL decay [4,108], is more a cause of damage to fine-grained limestone than salts washed by the rain [119]. On crystallization, salts generate stresses within pores of the sediment, which may be in the range of 2 to 20 N/mm^2 [120].

5.5. Color

Color is caused by oxidizing or reducing processes at the time of sedimentation. Oxidation during the process of fragmentation might have changed the color of LGL from an original bluish-grey to yellow and ochre-brown, as illustrated by the blue lenticular patches at Msida [81,82]. Ferric solutions entering along cracks, marked with yellow bands on either side, create a contrast with the original green-grey calcite matrix [81]. The color changed from bluish-green to yellow due to post-depositional oxidation resulting from water flowing through the cracks.

Minerals such as quartz, feldspars, augite, mica may be of igneous origin. Terrigenous components in LGL are rare or sporadic and are very small in size, mainly below 0.1 mm. This makes it difficult to accurately determine under a microscope the type of feldspars (plagioclase and K-feldspar). Quartz grains are mostly monocrystalline and some of them have undulose extinction. Other LGL-forming clay minerals are formed by the weathering of non-clay minerals. The color of pure calcium carbonate and pure clay minerals is white with occasional tints of grey and green. The introduction of pigments such as ferrous-ferric iron hydroxides or limonite minerals can generate green or yellow-ochre hues, respectively. Soluble hydrocarbons give a grey-to-black color. Iron-based minerals are more abundant in second-quality LGL. Such minerals have the strongest pigment. These pigments are usually unstable if exposed to light and weathering. Most of the iron has been formed

either by precipitation or during geological processes related or unrelated to lithification. From thin section studies, iron minerals have been washed into the formation as iron in solution or freed through decaying organic material. There is a reasonable correlation of color with the Fe_2O_3 content.

Color changes according to whether the dimension stones are freshly cut or weathered. In the former, color is important as a quality criterion. Color on drying is an imperative visual consideration when selecting building stones. It is important that dimension stones in buildings, in particular monumental and official structures, weather as desired.

5.6. Bioturbation

Formed within soft unconsolidated sediments, burrows exhibit patterns, shapes and well-defined ichnofabrics [121]; their compaction can be computed in terms of Ricken [122]. Bioturbation is a process whereby sediments are remixed by organisms, affecting the porosity and permeability of the host sediment [123]. Bioturbated and non-bioturbated areas have an impact on the weathering of the fabric [84]. Bio-retexturing is a process which destroys the primary depositional fabrics and masks inorganic process-related structures [123]. Photos taken on site indicate bio-retexturing and weathering in inferior LGL. Burrowing activity introduces unlithified sediment of variable permeability in the host rock [84,124]. The XRF and XRD analyses indicate that the mineralogy of burrow infill is quantitatively different from the host rock. When rich in goethite, the infills have a characteristic dark yellow ochre-like color.

6. Conclusions

Composed of calcium carbonate limestone of predominantly medium purity (only few first-quality lithobeds are of high purity), LGL was subject to varying lithification and compaction processes during diagenesis. LGL with a high quartz and clay content is of the inferior lithotype (and marginally more expensive on the tungsten carbide tips used in circular saws to quarry [79]). It is less durable, although its CS is comparable to the first-quality lithotype. The following conclusions were drawn [40]:

1. IR content is indicative of the quality of LGL

Bulk chemistry and mineralogical show that non-carbonate and clay content increase with decreasing quality in LGL; thus a lower IR content suggests higher-quality LGL. An anomaly is present in the designation of the quality of two samples (Q1_8 and Q1_9) based on the visual presence of bioturbation. An IR threshold of 5% was introduced in 1994 by the author, then a Minerals Planning Officer within the Planning Authority (Malta), as a benchmark to evaluate the quality of the mineral resources prior to issuing development planning consent for new LGL quarries or extensions to existing sites. An IR content of <5% denotes first-quality LGL; IR content $\geq$5% is indicative of inferior lithotypes. The reliability of this rudimentary mineralogical method as a mode of quality control—an empirical grounding to the alternative of visual assessment—was confirmed by research carried out several years later [125].

2. Bioturbation is a reliable method to assess the quality LGL

Bio-retexturing introduces unlithified sediment of variable permeability into the host rock [124]. The mineralogy of burrow infill is quantitatively different from the host rock. Sometimes, such burrows are richer in goethite. Bioturbation is pronounced in the inferior lithotype [84].

3. First-quality LGL is more porous than inferior lithotypes

Measuring porosity is a traditional field method used to differentiate between two lithotypes. The inferior lithotype is richer in clay minerals, which may be a cause of weakness in the fabric, reducing its durability. This research established that in first-quality LGL, the movement of water through the matrix encourages the growth of the post-depositional interlocking calcite crystals whose physico-mechanical bonding enhances the durability of the lithotype.

4. Other correlations

Interpolation of results indicates that there is a correlation between density and color, density and CS, and color and Fe_2O_3 content.

Research on restoration of built heritage focuses on employing techniques that prohibit the ingress of moisture into the fabric. This approach ignores self-sustaining reactions—both mineralogical and otherwise—which continue to take place within the fabric. Studying the mechanics and processes inherent to the nature of the fabric is vital in order to understand and predict the likely behavior of the fabric when a particular restoration technique is used. Interfering with natural weathering processes hinders the course of the action of the elements.

Funding: This research was funded through a scholarship from the Oil Exploration Directorate, Office of the Prime Minister, Malta, to undertake postgraduate studies under the academic supervision of Hugh Martyn Pedley at the University of Leicester, UK.

Institutional Review Board Statement: Not applicable.

Informed Consent Statement: Not applicable.

Data Availability Statement: Not applicable.

Acknowledgments: The author would like to thank his academic tutor Hugh Martyn Pedley for sharing his invaluable academic and field experience on the geology of the Maltese Islands; the late Anselm Dunham (former Head of the Department of Geology, University of Leicester) for his methodical approach in industrial mineralogy and his unwavering scholarly advice; Godwin Debono and Saviour Xerri (both formerly of the Oil Exploration Directorate, Office of the Prime Minister, Malta); Godwin Cassar and the late Fredrick Camilleri (former Director General and Head of the Minerals Planning Unit, Planning Authority, Malta); Alex Torpiano (Dean, Faculty of the Built Environment, University of Malta; then Head of the Building and Civil Engineering Department at the same university); and the late Salvatore Bondin (former President of Għaqda Sidien tal-Barrieri, Quarry Owners Association, Malta), a third generation quarryman with over 60 years of experience in open-pit mining in Malta. A note of gratitude to Elena Koleva-Rekalova (Department of Paleontology, Geological Institute Strashimir Dimitrov, Bulgarian Academy of Sciences) for re-examining the thin-sections, for the microphotographs reproduced in Figures 10 and 11, and for her invaluable comments on the draft version of this paper, and to Elena Marrocchino and Carmela Vaccaro (both of the Department of Physics and Earth Sciences, University of Ferrara) who, as Guest Editors, invited this contribution to the Special Issue on "Geochemical, Mineralogical, and Petrographical Applications to Environment and Cultural Heritage" published in *Minerals*. A final note to thank Radostina Atanassova (Scientific Secretary, Geological Institute Strashimir Dimitrov, Bulgarian Academy of Sciences) and the three anonymous referees of the journal for their comments and suggestions.

Conflicts of Interest: The author declares no conflict of interest.

References

1. Coleridge, S.T. *The Notebooks of Samuel Taylor Coleridge*, 2nd ed.; Coburn, K., Ed.; Routledge & Kegan Paul: London, UK, 1962; Volume 1804–1808.
2. Blouet, B. *The Story of Malta*; Faber and Faber: London, UK, 1967.
3. Palmer, R. Coleridge, material culture, and Malta. *ANQ A Q. J. Short Artic. Notes Rev.* **2014**, *27*, 5–12. [CrossRef]
4. Quintin d'Autin, J. *The Earliest Description of Malta*; DeBono Enterprises: Sliema, Malta, 1980.
5. Seddall, H. *Malta: Past and Present: Being a History of Malta from the Days of the Phoenicians to the Present Time*; Chapman and Hall: London, UK, 1870.
6. Oil Exploration Directorate. *Geological Map of the Maltese Islands (Sheet 1, Malta; Sheet 2, Gozo), 1:25,000*; British Geological Survey: Keyworth, UK, 1993.
7. Childe, C.V. *The Dawn of European Civilisation*; Kegan Paul: London, UK, 1957.
8. Evans, J.D. *The Prehistoric Antiquities of the Maltese Islands: A Survey*; Athlone Press: London, UK, 1971.
9. Renfrew, A.C. *Before Civilisation*; Cape: London, UK, 1973.
10. Trump, D.H. Megalithic architecture in Malta. In *Antiquity and Man: Essays in Honour of Glyn Daniel*; Evans, J.D., Cunliffe, B., Renfrew, C., Eds.; Thames and Hudson: London, UK, 1981; pp. 128–140.
11. Cherry, J.F. The first colonisation of the Mediterranean Islands: A review of recent research. *J. Medit. Archaeol.* **1990**, *3*, 145–221.

12. UNESCO. World Heritage List: Megalithic Temples of Malta. Available online: http://whc.unesco.org/en/list/132 (accessed on 21 January 2021).
13. Bianco, L. Architectural ruins: Geoculture of the anatomy of buildings as illustrated by Casa Ippolito, Malta. *Herit. Sci.* **2021**, *9*, 1–19. [CrossRef] [PubMed]
14. UNESCO. World Heritage List: Ħal Saflieni Hypogeum. Available online: http://whc.unesco.org/en/list/130 (accessed on 21 January 2021).
15. Heritage Malta. St. Paul's Catacombs. Available online: https://heritagemalta.org/st-pauls-catacombs/ (accessed on 16 March 2021).
16. Bonanno, A. *Malta: Phoenician, Punic, and Roman*; Midsea Books: Sta Venera, Malta, 2005.
17. De Giorgio, R. *A City by an Order*, 2nd ed.; Progress Press Co. Ltd.: Valletta, Malta, 1985.
18. UNESCO. World Heritage List: City of Valletta. Available online: http://whc.unesco.org/en/list/131 (accessed on 21 January 2021).
19. Hughes, Q. *The Building of Malta during the period of the Knights of St John of Jerusalem*; Alec Tiranti: London, UK, 1967.
20. Mahoney, L. *5000 years of Architecture in Malta*; Valletta Publishing: Valletta, Malta, 1996.
21. De Lucca, D. *Mdina: A History of Its Urban Space and Architecture*; Said International: Valletta, Malta, 1995.
22. Hoppen, A. *The Fortification of Malta by the Order of St John 1530–1798*; Scottish Academic: Edinburgh, UK, 1979.
23. Spiteri, S. *Fortresses of the Cross*; Print Services Ltd.: Qormi, Malta, 1994.
24. Blouet, B.W. The Changing Landscape of Malta during the Rule of the Order of St John of Jerusalem 1530–1798. Ph.D. Thesis, University of Hull, Hull, UK, 1964.
25. Bianco, L.; Cardona, K. Seventeenth-century building engineering in the central Mediterranean: A case study from Malta. *Terra Sebus. Acta Musei Sabesiensis* **2020**, *12*, 329–353.
26. Fergusson, J. *History of the Modern Styles of Architecture: Being a Sequel to the Handbook of Architecture*; John Murray: London, UK, 1862.
27. Bianco, L. A geohistorical retrospective analysis of cultural heritage buildings: The case of Mosta Dome, Malta. *GeoJournal* **2019**, *84*, 291–302. [CrossRef]
28. Abela, G.F. *Della Descrittione di Malta isola nel Mare Siciliano: Con le sue Antichità, ed Altre Notizie*; Paolo Bonacota: Valletta, Malta, 1647.
29. Bianco, L. Geocultural activity in seventeenth and eighteenth century Malta. *GeoJournal* **1999**, *48*, 337–340. [CrossRef]
30. PEUPLIER. Hagar Qim. Available online: http://www.flickr.com/photos/peuplier/3019403075/ (accessed on 15 February 2021).
31. Mamo, J. Marbles and limestones of Malta. *Sands Clays Miner.* **1936**, *2*, 83–88.
32. Bruno, B. *L'Arcipelago Maltese ill Eta' Romana e Bizalltilla*; Edipuglia: Bari, Italy, 2004.
33. Ellul, M. Malta limestone goes to Europe: Use of Malta stone outside Malta. In *60th Anniversary of the Malta Historical Society: A Commemoration*; Grima, J.F., Ed.; Veritas Press: Zabbar, Malta, 2010; pp. 371–406.
34. Lino Bianco and Associates. *Retention of the Status quo Regarding the Exportation of Maltese Stone: Study for the Ministry for Economic Services, Malta*; Lino Bianco & Associates: Ħamrun, Malta, 2000; Available online: https://www.um.edu.mt/library/oar/bitstream/123456789/45116/1/Case_for_the_retention_of_the_status_quo_regarding_the_exportation_of_Maltese_stone.pdf (accessed on 22 January 2021).
35. Bianco, L. *Internal Policy on the Utilisation of Malta Stone*; Ministry for Resources and Infrastructure: Beltissebħ, Malta, 2002.
36. Cassar, J.; Torpiano, A.; Zammit, T.; Micallef, A. Proposal for the nomination of Lower Globigerina Limestone of the Maltese Islands as a "Global Heritage Stone Resource". *J. Int. Geosci.* **2017**, *40*, 221–231. [CrossRef]
37. Hodul, J.; Žižková, N.; Drochytka, R.; Borg, R.P. Influence of crystallization admixture on mechanical parameters and microstructure of polymer-cement mortars with waste limestone. *Solid State Phenom.* **2019**, *296*, 27–34. [CrossRef]
38. Hodul, J.; Žižková, N.; Borg, R.P. The influence of crystalline admixtures on the properties and microstructure of mortar containing by-products. *Buildings* **2020**, *10*, 146. [CrossRef]
39. University of Malta. *Annual Report 2019*; Marketing, Communications & Alumni Office: Msida, Malta, 2021; Available online: https://www.um.edu.mt/__data/assets/pdf_file/0004/455647/annualreport2019.pdf (accessed on 17 March 2021).
40. Bianco, L. Some Factors Controlling the Quality of Lower Globigerina Building Stone of Malta. Master's Thesis, University of Leicester, Leicester, UK, 1993.
41. Bianco, L. Techniques to determine the provenance of limestone used in Neolithic architecture of Malta. *Rom. J. Phys.* **2017**, *62*, 901.
42. Fort, R.; Alvarez de Buergo, M.; Perez-Monserrat, E.M.; Varas, M.J. Characterisation of monzogranitic batholiths as a supply source for heritage construction in the northwest of Madrid. *Eng. Geol.* **2010**, *115*, 149–157. [CrossRef]
43. Torok, A.; Prikryl, R. Current methods and future trends in testing, durability analyses and provenance studies of natural stones used in historical monuments. *Eng. Geol.* **2010**, *115*, 139–142. [CrossRef]
44. Bianco, L. Natural Weathering Processes Affecting Limestone. *The Times [of Malta] Building and Architecture Supplement*, 7 August 1994; pp. 10–11.
45. Spratt, T.A.B. On the geology of the Maltese Islands. *Proc. Geol. Soc.* **1843**, *4*, 225–229.
46. Spratt, T.A.B. *On the Geology of Malta and Gozo*; Malta Mail Office: Valletta, Malta, 1852.
47. Adams, A.L. Outline of the geology of the Maltese Islands. *Ann. Mag. Nat. Hist.* **1864**, *14*, 1–11.

48. Murray, J. The Maltese Islands, with special reference to their geological structure. *Scott. Geogr. Mag.* **1890**, *6*, 449–488. [CrossRef]
49. Rizzo, C. *Report on the Geology of the Maltese Islands: Including Chapters on Possible Ground-Water-Tables and Prospecting for Mineral-oil and Natural-Gas*; Government Printing Office: Valletta, Malta, 1932.
50. Hyde, H.P.T. *Geology of the Maltese Islands*; Lux Press: Valletta, Malta, 1955.
51. Zammit-Maempel, G. *An Outline of Maltese Geology*; Progress Press: Birkirkara, Malta, 1977.
52. House, M.R.; Dunham, K.C.; Wigglesworth, J.C. Geology of the Maltese Islands. In *Malta: Background for Development*; Bowen-Jones, H., Dewdney, J.C., Fisher, W.B., Eds.; University of Durham: Newcastle, UK, 1961; pp. 24–33.
53. Felix, R. *Oligo-Miocene Stratigraphy of Malta and Gozo*; H. Veenman and B.V. Zonen: Wageningen, The Netherlands, 1973.
54. Pedley, H.M. The Oligo-Miocene Sediments of the Maltese Islands. Ph.D. Thesis, University of Hull, Hull, UK, 1975.
55. Pedley, H.M.; House, M.R.; Waugh, B. The geology of the Pelagian Block: The Maltese Islands. In *The Ocean Basins and Margins*; Nairn, A.E.M., Kanes, W.H., Stehli, F.G., Eds.; Springer: Boston, MA, USA, 1978; Volume 4B, pp. 417–433.
56. Pedley, H.M. A new lithostratigraphical and palaeoenvironmental interpretation for the Coralline Limestone formations (Miocene) of the Maltese Islands. *Inst. Geol. Sci. Overseas Geol. Min. Resour.* **1978**, *54*, 273–291.
57. Burollet, P.F. Petroleum geology of the Western Mediterranean Basin. In *The Exploration for Petroleum in Europe and North Africa*; Institute of Petroleum: London, UK, 1969; pp. 19–30.
58. Burollet, P.F. Importance des facteurs salifères dans la tectonique tunisienne. In *Livre Jubilaire de M. Solignac*; Annales des Mines et de la Geéologie; Service Geéologique de Tunisie: Tunis, Tunisia, 1973; Volume 26, pp. 111–120.
59. Burollet, P.F.; Mugniot, J.M.; Sweeney, P. The geology of the Pelagian Block: The Margins and Basins off Southern Tunisia and Tripolitania. In *The Ocean Basins and Margins*; Nairn, A.E.M., Kanes, W.H., Stehli, F.G., Eds.; Springer: Boston, MA, USA, 1978; pp. 331–359.
60. Morelli, C.; Gantar, G.; Pisani, M. Bathymetry, gravity and magnetism in the Strait of Sicily and the Ionian Sea. *Boll. Di. Geofis. Teor. Ed. Appl.* **1975**, *17*, 39–58.
61. Spratt, T.A.B. On the Bone-Caves near Crendi, Zebbug, and Melliha, in the Island of Malta. *Q. J. Geol. Soc.* **1867**, *23*, 283–297. [CrossRef]
62. Giannelli, L.; Salvatorini, G. I foraminiferi planctonici dei sediment terziari dell'arcipelago Maltese. I. Biostratigrafia dell Globigerina Limestone. *Atti Della Soc. Toscana Sci. Nat. Mem. Ser. A* **1972**, *79*, 49–74.
63. Pedley, H.M. Miocene sea-floor subsidence and later subaerial solution subsidence structures in the Maltese Islands. *Proc. Geol. Assoc.* **1974**, *85*, 533–547. [CrossRef]
64. Pedley, H.M.; House, M.R.; Waugh, B. The geology of Malta and Gozo. *Proc. Geol. Assoc.* **1976**, *87*, 325–341. [CrossRef]
65. Baldassini, N.; Di Stefano, A. Stratigraphic features of the Maltese Archipelago: A synthesis. *Nat. Hazards* **2017**, *86*, 203–231. [CrossRef]
66. Baldassini, N.; Mazzei, R.; Foresi, L.M.; Riforgiato, F.; Salvatorini, G. Calcareous plankton bio-chronostratigraphy of the Maltese Lower Globigerina Limestone member. *Acta Geol. Pol.* **2013**, *63*, 105–135. [CrossRef]
67. Foresi, L.M.; Mazzei, R.; Salvatorini, G.; Donia, F. Biostratigraphy and chronostratigraphy of the Maltese Lower Globigerina Limestone Member (Globigerina Limestone Formation): New preliminary data based on calcareous plankton. *Boll. Della. Soc. Paleontol. Ital.* **2007**, *46*, 175–181.
68. Challis, G.R. Miocene echinoid biofacies of the Maltese Islands. *Annales Géologiques des Pays Helléniques Tome Hors Série* **1979**, *1*, 253–261.
69. Bennett, S.M. Palaeoenvironmental Studies in Maltese Mid-Tertiary Carbonates. Ph.D. Thesis, University of London, London, UK, 1980.
70. Carbone, S.; Grasso, M.; Lentini, F.; Pedley, H.M. The distribution and palaeoenvironmental of early Miocene phosphorites of southeast Sicily and their relationship with the Maltese phosphorites. *Palaeogeogr. Palaeoclimatol. Palaeoecol.* **1987**, *58*, 35–53. [CrossRef]
71. Rose, E.P.F.; Pratt, S.K.; Bennett, S.M. Evidence for Sea-Level Changes in the Globigerina Limestone formation (Miocene) of the Maltese Islands. *Paleontol. I Evol.* **1992**, *24–25*, 265–276.
72. Bennett, S.M. A transgressive carbonate sequence spanning the Paleogene Neogene boundary on the Maltese Islands. *Ann. Géol. Pays Helléniques* **1979**, *1*, 71–80.
73. Continentalshelf.gov.mt. Geological Map of the Maltese Islands. Available online: https://continentalshelf.gov.mt/en/Pages/Geological-Map-of-the-Maltese-Islands.aspx (accessed on 21 April 2021).
74. Pedley, H.M.; Bennett, S.M. Phosphorites, hardgrounds and syndepositional subsidence: A paleoenvironmental model from Miocene of the Maltese Islands. *Sediment. Geol.* **1985**, *45*, 1–34. [CrossRef]
75. Rehfeld, U.; Janssen, A.W. Development of phosphatized hardgrounds in the Miocene Globigerina Limestone of the Maltese Archipelago, including a description of Gamopleura melitensis sp. nov. (Gastropoda, Euthecosomata). *Facies* **1995**, *33*, 91–106. [CrossRef]
76. Colson, C.; Colson, C.H. The 160-ton hydraulic crane at Malta dockyard extension works. *Minutes Proc. Inst. Civ. Eng.* **1893**, *114*, 284–288.
77. Adams, A.L. *Notes of a Naturalist in the Nile Valley and Malta: A Narrative of Exploration and Research in Connection with the Natural History, Geology, and Archaeology of the Lower Nile and Maltese Islands*; Edmonston and Douglas: Edinburgh, UK, 1870.
78. Bianco, L. The industrial minerals of the Maltese islands: A general introduction. *Hyphen* **1995**, *7*, 111–118.

79. Bondin, S.; Former President of the Softstone Quarry Association, Mqabba, Malta. Personal Communication, 1992.
80. Camilleri, D.H. Globigerina limestone as a structural material. *Architect* **1988**, *9*, 17–25.
81. Bianco, L. Mineralogy and geochemistry of blue patches occurring in the *Globigerina* Limestone Formation used in the architecture of the Maltese Islands. *C. R. L'académie Bulg. Sci.* **2017**, *70*, 537–544.
82. Bianco, L. Petrological characteristics of blue lenticular patches occurring in the lower globigerina building limestone of Malta. *Rom. J. Mater.* **2018**, *48*, 115–120.
83. Planning Authority. Available online: http://geoserver.pa.org.mt/publicgeoserver (accessed on 1 February 2021).
84. Bianco, L. Bio-retexturing in limestone used in the built heritage of Malta. *Rom. Rep. Phys.* **2017**, *69*, 802.
85. Bianco, L. Limestone replacement in restoration: The case of the Church of Santa Maria (Birkirkara, Malta). *Int. J. Conserv. Sci.* **2017**, *8*, 167–176.
86. Montebello, T.; Sculptor, Restoration of Church of Santa Maria, Birkirkara, Malta. Personal Communication, 1992.
87. Dean, W.E. Determination of carbonate and organic matter in calcareous sediments and sedimentary rocks by loss on ignition: Comparison with other methods. *J. Sediment. Petrol.* **1974**, *44*, 242–248.
88. Fitton, G. X-ray fluorescence spectrometry. In *Modern Analytical Geochemistry: An Introduction to Quantitative Chemical Analysis for Earth, Environmental and Material Scientists*; Gill, R., Ed.; Longman: Harlow, UK, 1997; pp. 97–115.
89. Drever, J.I. The preparation of oriented clay mineral specimens for X-ray diffraction analysis by a filter-membrane peel technique. *Am. Mineral.* **1973**, *58*, 553–554.
90. Koleva-Rekalova, E. Petrographical Descriptions of Thin Sections from the Lower Globigerina Limestone Member from Malta. Unpublished work. 2017.
91. Dunham, R.J. Classification of carbonate rocks according to depositional texture. In *Classification of Carbonate Rocks—A Symposium*; Ham, W.E., Ed.; American Association of Petroleum Geologists: Tulsa, OK, USA, 1962; Memoir 1; pp. 108–121.
92. Pye, K. Forensic examination of rocks, sediments, soils and dusts using scanning electron microscopy and X-ray chemical microanalysis. In *Forensic Geoscience: Principles, Techniques and Applications*; Pye, K., Croft, D.J., Eds.; Geological Society: London, UK, 2004; pp. 103–122.
93. Reed, S.J.B. *Electron Microprobe Analysis and Scanning Electron Microscopy in Geology*; Cambridge University Press: Cambridge, UK, 2005.
94. Cnudde, V.; Cwirzen, A.; Masschaele, B.; Jacobs, P.J.S. Porosity and microstructure characterization of building stones and concretes. *Eng. Geol.* **2009**, *103*, 76–83. [CrossRef]
95. Yan, Z.; Chen, C.; Fan, P.; Wang, M.; Fang, X. Pore structure characterization of ten typical rocks in China. *Electron. J. Geotech. Eng.* **2015**, *20*, 479–494.
96. Tucker, M.E. *Sedimentary Petrology: An Introduction*, 3rd ed.; Blackwell Scientific Publications: Oxford, UK, 2001.
97. Camilleri, D.H. *Structural Integrity Handbook: Building-Regulations 2000*; Building Industry Consultative Council: Floriana, Malta, 2000; Available online: http://www.dhiperiti.com/wp-content/uploads/2013/10/2.Structural-Integrity-Handbook-Building-Regulations-20006.pdf (accessed on 17 March 2021).
98. Centre Technique de Matériaux Naturels de Construction. *Study on Characteristic Compressive Strength of Natural Stone Masonry Made with General Purpose Mortar*; Centre Technique de Matériaux Naturels de Construction: Paris, France, 2015.
99. Camilleri, D.H. Malta's heritage in stone: From temple builders to Eurocodes 6/8. *Mason. Int.* **2019**, *31*, 49–67.
100. Vasanelli, E.; Colangiuli, D.; Calia, A.; Sileo, M.; Aiello, M.A. Ultrasonic pulse velocity for the evaluation of physical and mechanical properties of a highly porous building limestone. *Ultrasonics* **2015**, *60*, 33–40. [CrossRef]
101. Anonymous. Classification of rocks and soils for engineering geological mapping. Part I—Rock and soil materials. *Bull. Int. Assoc. Eng. Geol.* **1979**, *19*, 364–371. [CrossRef]
102. Cox, F.C.; McC Bridge, D.; Hull, J.H. *Procedure for the Assessment of Limestone Resources: Mineral Assessment Report 30*; Institute of Geological Sciences: London, UK, 1977.
103. Torrero, E.; Sanz, D.; Arroyo, M.N.; Navarro, V. The Cathedral of Santa Maria (Cuenca, Spain): Principal stone characterization and conservation status. *Int. J. Conserv. Sci.* **2015**, *6*, 625–632.
104. Balog, A.-A.; Cobirzan, N.; Mosonyi, E. Analysis of limestones from heritage buildings as damage diagnostics. *Rom. Rep. Phys.* **2016**, *68*, 353–361.
105. Choquette, P.W.; Pray, L.C. Geologic nomenclature and classification of porosity in sedimentary carbonates. *Bull. Am. Assoc. Pet. Geol.* **1970**, *54*, 207–250.
106. Robertson, J.C. *Report on the Possibility of Increasing the Fresh Water Supply and of Utilising the Sewage for Crop Irrigation in Malta*; Government Printing Office: Valletta, Malta, 1917.
107. Morris, T.O. *The Water Supply Resources of Malta*; Government of Malta: Valletta, Malta, 1952.
108. De Boisgelin, L. *Ancient and Modern Malta*; Richard Philips: London, UK, 1805.
109. Galea, R.V. Geology of the Maltese archipelago. In *Malta and Gibraltar Illustrated*; Macmillan, A., Ed.; W.H. and L. Collingridge: London, UK, 1915; pp. 173–182.
110. Building Research Station. *The Maltese Islands: Use of Limestone for Building*; Department of Scientific and Industrial Research, Building Research Station: Watford, UK, 1958.
111. Building Research Station. *Maltese Limestones: Relation of Durability to Laboratory-Measured Properties and Efficacy of Silicone Treatments: Note No. C965*; Department of Scientific and Industrial Research, Building Research Station: Watford, UK, 1963.

112. Building Research Station. *The Maltese Islands: Properties and Behaviour of Local Limestone: Internal Note 6*; Department of Scientific and Industrial Research, BRS: Watford, UK, 1964.
113. Fitzner, B.; Heinrichs, K.; Volker, M. Model for salt weathering in Maltese Globigerina limestone. In *Origin, Mechanisms and Effects of Salt on Degradation of Monuments in Marine and Continental Environments*; Zezza, F., Ed.; European Commission: Bari, Italy, 1997; pp. 333–344.
114. Sandrolini, F.; Franzoni, E.; Cuppini, G. Predictive diagnostics for decayed ashlars substitution in architectural restoration in Malta. *Mater. Eng.* **2000**, *11*, 323–337.
115. Koleva-Rekalova, E.; Bianco, L. Importance of optical microscopic investigation in provenance studies and quality characteristics of both historical and natural Lower Globigerina building limestone of Malta. *Rev. Bulg. Geol. Soc.* **2018**, *79*, 93–94.
116. Ellul, M.; Antiquities Division, Public Works Department, Floriana, Malta; University of Malta, Msida, Malta. Personal Communication, 1992.
117. Rossi-Manaresi, R.; Tucci, A. Pore structure and the disruptive or cementing effect of salt crystallization in various types of stone. *Stud. Conserv.* **1990**, *36*, 53–58.
118. Leeder, M.R. *Sedimentology: Process and Product*, 1st ed.; Chapman & Hall: London, UK, 1982; reprinted 1994.
119. Kozlowski, R.; Magiera, J.; Weber, J.; Haber, J. Decay and conservation of Pinczow porous limestone. *Stud. Conserv.* **1989**, *35*, 205–221. [CrossRef]
120. Ollier, C.D. *Weathering Geomorphology Texts*; Oliver & Boyd: Edinburgh, UK, 1984.
121. Bromley, R.G. *Trace Fossils. Biology, Taphonomy and Applications*; Chapman & Hall: London, UK, 1996.
122. Ricken, W. The carbonate compaction law: A new tool. *Sedimentology* **1987**, *34*, 571–584. [CrossRef]
123. Gingras, M.K.; Baniak, G.; Gordon, J.; Hovikoski, J.; Konhauser, K.O.; La Croix, A.; Lemiski, R.; Mendoza, C.; Pemberton, S.G.; Polo, C.; et al. Porosity and permeability in bioturbated sediments. In *Trace Fossils as Indicators of Sedimentary Environments*; Knaust, D., Bromley, R.G., Eds.; Elsevier: Amsterdam, The Netherlands, 2012; pp. 837–868.
124. Pedley, H.M. Bio-retexturing: Early diagenetic fabric modifications in outer-ramp settings—A case study from the Oligo-Miocene of the Central Mediterranean. *Sediment. Geol.* **1992**, *79*, 173–188. [CrossRef]
125. Cassar, J.; Vella, A.J. Methodology to identify badly weathering limestone using geochemistry: Case study on the Lower Globigerina Limestone of the Maltese Islands. *Q. J. Eng. Geol. Hydrogeol.* **2003**, *36*, 85–96. [CrossRef]